Supporting Information

Catalytic Oxidation of Methane into Methanol over Copper-Exchanged Zeolites with Oxygen at Low Temperature

Karthik Narsimhan, Kenta Iyoki, Kimberly Dinh, Yuriy Román-Leshkov*

Department of Chemical Engineering, Massachusetts Institute of Technology, 77 Massachusetts Ave, Cambridge, Massachusetts 02139, United States

* Correspondence to: yroman@mit.edu

Table of Contents

Materials and Methods

Materials

***Commercial zeolites*.** Zeolites MOR (mordenite, CBV21A, Si/Al = 10), ZSM-5 (MFI, CBV2314, Si/Al = 11.5), BEA (beta, CP814E, Si/Al = 12.5), FER (ferrierite, CP914C, Si/Al = 10), and Y (FAU, CBV100, Si/Al = 5.1) were purchased from Zeolyst International. MCM-41 (Aluminosilicate Al-MCM-41, Si/Al = 12) was purchased from ACS Materials. All zeolites were in the ammonium form except for Y and MCM-41, which were in the sodium form.

Zeolite Synthesis

***Synthesis of SSZ-13 (CHA*):** sodium hydroxide (99.99%, Sigma-Aldrich) was dissolved in H_2O and mixed with N,N,N-trimethyl-1-adamantanamine hydroxide solution (Ada, 25 wt % in H_2O, Sachem) followed by the addition of aluminum hydroxide (80.3 wt % $Al(OH)_3$, SPI Pharma 0250) to obtain a colorless solution. After the addition of colloidal silicon dioxide (SiO_2) (Ludox® LS-30), the colorless solution was stirred at room temperature for 2 h. The final composition of the mixture was 0.1 Na_2O: 0.033 Al_2O_3: 1.0 SiO_2: 44 H_2O: 0.1 $(Ada)_2O$. This mixture was transferred to a 23-mL Teflon-lined stainless steel autoclave (No. 4749, Parr Instruments) and was then subjected to hydrothermal treatment at 433 K for 4 days in an oven under autogenous pressure and rotation (60 rpm). After hydrothermal treatment, the product was separated from the mother liquor by centrifugation, washed several times with distilled H_2O, and dried at 393 K. SSZ-13 samples were calcined under dry air (Dry Size 300, Airgas) with the following temperature profile: heat 1 K min^{-1} to 423 K and hold for 2 h at 423 K, then heat 1 K min^{-1} to 623 K and hold for 2 h at 623 K, and lastly heat 1 K min^{-1} to 853 K and hold for 10 h.

Synthesis of SAPO-34 (CHA): Aluminum oxide (Al_2O_3) (Catapal® B) and colloidal silicon dioxide (SiO_2) (Ludox® AS-40) were added to a mixture of phosphoric acid (85 wt %, Sigma-Aldrich) and H_2O. Diethylamine (DEA, 99.5%, Sigma-Aldrich) was added to the mixture to obtain a gel with the composition of 0.8 P_2O_3: Al_2O_3: 0.6 SiO_2: 50 H_2O: 2 DEA. The mixture was stirred for 0.5 h and then subjected to hydrothermal treatment at 423 K for 7 days with 60 rpm rotation. After hydrothermal treatment, the product was separated from the mother liquor by centrifugation, washed several times with distilled H_2O, and dried at 393 K. SAPO-34 samples were calcined under dry air (Dry Size 300, Airgas) with the same temperature profile stated for SSZ-13 samples.

***Synthesis of pure silica BEA*:** Si-BEA was synthesized based on a procedure reported by Camblor et.al.[1] Aqueous tetraethylammonium hydroxide (27.169 g, 35 wt% in H_2O, Sigma-Aldrich) and tetraethyl orthosilicate (24.160 g, 99%, Sigma Aldrich) were added to a Teflon [polytetrafluoroethylene (PTFE)] dish and stirred at 250 rpm at room temperature for 90 min. Deionized H_2O (15 mL) was added and the solution was left uncovered on the stir plate for 12 h to reach a total mass of 33.046 g after evaporation of ethanol and some of the H_2O. Next, hydrofluoric acid (2.627 g, 48wt% in H_2O, > 99.99% trace metals basis, Sigma-Aldrich) was added drop wise and mixed using a PTFE spatula, resulting in a thick gel. Additional H_2O was added to aid homogenization and the sol-gel was allowed to evaporate to 33.848 g. The final molar composition was 1 SiO_2:0.56 TEAOH:0.56 HF:7.5 H_2O. The gel was transferred to a 45 mL PTFE-lined stainless steel autoclave and heated to 413 K for 7-20 days under static

conditions. The product was separated from the mother liquor by filtration, washed with distilled H_2O, and dried at 373 K. The zeolite was calcined under dry air (Dry Size 300, Airgas) with the same temperature profile stated for SSZ-13 samples.

Synthesis of pure silica MFI: Si-MFI was synthesized based on a procedure reported by Persson et.al.[2] Aqueous tetrapropylammonium hydroxide (12.00 g, 1.0 M in H_2O, Sigma-Aldrich) and tetraethyl orthosilicate (5.00 g, 99%, Sigma Aldrich) were added to a Teflon [polytetrafluoroethylene (PTFE)] dish and stirred at 300 rpm at room temperature for 60 min. The molar composition was 1 SiO_2:0.5 TPAOH:22 H_2O. The gel was transferred to a 23 mL PTFE-lined stainless steel autoclave and heated to 453 K for 2 days under static conditions. The product was separated from the mother liquor by centrifugation, washed with distilled H_2O, and dried at 373 K. The zeolite was calcined under dry air (Dry Size 300, Airgas) with the same temperature profile stated for SSZ-13 samples.

Ion Exchange

Sodium exchange. The following procedure was used to ion-exchange all zeolites: 1 g of zeolite was stirred in 36 mL of 2.44 M sodium acetate (> 99%, Sigma-Aldrich) at 353 K for 4 h. Zeolites were subsequently filtered while hot and rinsed with 120 mL of deionized H_2O. Zeolites were then dried for 4 h at 393 K in a drying oven. The above procedure was repeated three times.

Copper exchange. The following procedure was used to ion-exchange all zeolites: 1 g of zeolite was stirred in 60 mL of 0.001 - 0.05 M solutions of copper (II) acetate monohydrate (> 99%, Sigma-Aldrich) at room temperature overnight. The suspension was then filtered at room temperature and rinsed with 300 mL of deionized H_2O. The zeolite was dried overnight at 393 K in a drying oven and subsequently calcined under dry air (Dry Size 300, Airgas) at 823 K for 5 h with a heating ramp of 1 K min^{-1}.

Incipient Wetness Impregnation

CuO_x-BEA. 0.23 g of a 0.23 M solution of copper (II) nitrate trihydrate (> 99%, Sigma-Aldrich) was added dropwise to 0.30 g of Si-BEA under vigorous stirring, yielding 1.1 wt% of CuO_x on the BEA zeolite. CuO_x-BEA was dried overnight at 383 K and then calcined at 853 K for 10 h under flowing dry air (Dry Size 300, Airgas) with a heating ramp of 1 K min^{-1}. The resultant zeolite had a gray color.

CuO_x-MFI. 0.239 g of a 0.241 M solution of copper (II) nitrate was added dropwise to 0.352 g of Si-MFI under vigorous stirring, yielding 1.1 wt% of CuO_x on the MFI zeolite. CuO_x-MFI was dried overnight and calcined in the same way as stated for CuO_x-BEA. The resultant zeolite had a gray color.

Characterization

Elemental analysis. Copper (Cu), sodium (Na), aluminum (Al), and iron (Fe) contents were determined using inductively coupled plasma mass spectrometry (ICP-MS) (Agilent 7900). 2.0 –

10.0 mg of zeolite were placed in a polyethylene microfuge tube (1.5 mL) and digested in 0.1 mL hydrofluoric acid (48 wt %, trace metals basis, Sigma-Aldrich) for 3 h. The hydrofluoric acid solution was diluted to a total mass of 10.0 g using 2 wt % aqueous nitric acid (HNO_3) (veritas purity, GFS Chemicals). 0.10 g of this solution was then added to two solutions: 1) 0.10 g of 1 part per million (ppm) erbium in 2 wt% HNO_3 solution; 2) 9.80 g of 2 wt% HNO_3. The final concentration of each element was 10 parts per billion (ppb) erbium and between 10 to 300 ppb for Cu, Na, Al, and Fe. A five point calibration curve was built using the following ICP standard solutions: 1,000 ppm Cu in 2 wt% HNO_3, 1,000 ppm Al in 2 wt% HNO_3, 1,000 ppm Na in 2 wt% HNO_3, and 1,000 ppm Fe in 2 wt% HNO_3. All standard solutions were purchased from Sigma-Aldrich (TraceCERT).

Calculations of molar ratios Si/Al$_{tot}$ and Cu/Al$_{tot}$. The unit cell of a zeolite is given by:

$$H_x^+ Na_y^+ Cu_z^{2+} (AlO_2)_n^- (SiO_2)_m (H_2O)_k$$

where subscripts refer to the molar ratios of each component within the unit cell of a zeolite. Local charge balance was assumed to occur within the zeolite, requiring $x = n - 2z - y$.

From the unit cell given above, the mass balance of the unit cell is given by the following equation on a per gram zeolite basis:

$$1 = a\frac{g\ SiO_2}{g\ zeolite} + b\frac{g\ [AlO_2]^-}{g\ zeolite} + c\frac{g\ Cu^{2+}}{g\ zeolite} + d\frac{g\ Na^+}{g\ zeolite} + e\frac{g\ H^+}{g\ zeolite} + f\frac{g\ H_2O}{g\ zeolite}$$

where each coefficient represents the weight percent of each species. The weight percent of Al, Cu, and Na were directly calculated using ICP-MS, allowing b, c, and d to be determined. Converting the weight percentages of Al, Cu, and Na to mole percentages per gram zeolite, e was then calculated using the local charge balance of cations on the zeolite framework. The weight percentage of H_2O (f) was assumed to be equal to the weight percentage of H_2O in the zeolite framework unit cell (2 – 7 wt %).[3] The mass balance was then solved for the weight percentage of SiO_2 (a).

Si/Al$_{tot}$ was calculated by $\frac{Si}{Al_{tot}} = \frac{a}{b}\frac{m_{AlO2}}{m_{SiO2}} \times \frac{1\ mol\ Si}{1 mol\ SiO_2} \times \frac{1\ mol\ AlO_2}{1\ mol\ Al}$

where m_i is the molar mass of element i.

Cu/Al$_{tot}$ was calculated by $\frac{Cu}{Al_{tot}} = \frac{c}{b}\frac{m_{AlO2}}{m_{Cu}} \times \frac{1\ mol\ AlO_2}{1\ mol\ Al}$

Powder x-ray diffraction. The crystal structures of zeolite catalysts were determined from powder x-ray diffraction patterns collected using a Bruker D8 diffractometer using Cu-Kα radiation (λ = 1.5418 Å, 40 kV, 40 mA). Data were recorded in the range of 3-50 2θ with an angular step size of 0.02° and a counting time of 0.068 s per step.

Surface area and pore volume quantification. Nitrogen adsorption and desorption isotherms were measured on a Quantachrome Autosorb iQ apparatus at liquid nitrogen

temperature (77 K). Prior to the adsorption analysis, all samples were pelletized and degassed under vacuum for 12 h at 623 K. Micropore volume and total pore volume were determined from the amount of N_2 adsorbed at $P/P_0 = 0.01$ and $P/P_0 = 0.95$, respectively.

Transmission Electron Microscopy (TEM). Transmission electron microscopy was performed on a JEOL 2010F equipped with a field emission gun (FEG) operating at 200 kV. Magnifications of obtained images ranged from 50,000x to 100,000x.

Coupled in-situ UV-Vis-NIR Spectroscopy and Online Gas Chromatography. UV-Vis spectroscopy was performed on a Cary 5000 UV-Vis-NIR spectrometer (Agilent Technologies) equipped with a DiffusIR diffuse reflectance accessory (PIKE Technologies) and environmental chamber (HTV, PIKE Technologies) with a quartz window. Absolute reflectance was measured from 11,000 cm^{-1} to 52,600 cm^{-1} with a scan rate of 11,700 cm^{-1} min^{-1}. All spectra were normalized with respect to background spectra of hydrated Na-ZSM-5. The gas outlet from the environmental temperature chamber was connected to a gas chromatograph (Agilent Technologies, model 6890N) equipped with an S-bond column (Restek Rt-S-bond, 30 m, 0.25 mm ID, #19770) and flame ionization detector. The oven temperature was isothermal at 373 K for 10 min.

To conduct in-situ CH_4 oxidation reactions, the temperature was controlled using a PIKE PC Controlled Temperature Module. Cu-ZSM-5 (Cu/Al = 0.37) was ground into a fine powder before loading 10.0 mg into the sample cell. The flow of gases, including He (ultra high purity, Airgas), O_2 (ultra high purity, Airgas), 1% O_2/He (ultra high purity, Airgas), and CH_4 (research grade, Airgas) were controlled with independent mass flow controllers (Brooks Instruments LLC). H_2O (typically 3.2 kPa) was introduced into the gas stream using a saturator maintained at 298 K.

Catalytic CH_4 Oxidation Reactions

CH_4 oxidation reactions were conducted in a continuous, tubular flow reactor (stainless steel tube, O.D. 12.5 mm, wall thickness = 0.889 mm). The reactor tube was mounted inside of a single-zone furnace (850W / 115V, Applied Test Systems Series 3210). Temperature was controlled using a thermocouple (Omega, model TJ36-CASS-18U) mounted slightly downstream of the catalyst bed connected to a temperature controller (Digi-Sense model 68900-10). 2.0 g of zeolite particles (pelletized and sieved into 500–1000 μm particles) were packed between quartz wool plugs and rested on the thermocouple in the middle of the furnace heating zone. The flow of gases, including He (ultra high purity, Airgas), O_2 (ultra high purity, Airgas), 1% O_2 in N_2 (ultra high purity, Airgas), and CH_4 (research grade, Airgas) were controlled with independent mass flow controllers (Brooks Instruments LLC). H_2O (typically 3.2 kPa) was introduced into the gas stream using saturator maintained at 298 K. O_2 partial pressure entering the catalyst bed was monitored with an O_2 sensor (3000-G-115BTP, Omega Instruments) placed at the entrance of the furnace. Prior to reaction, the zeolite was usually calcined in situ under 50 mL min^{-1} flowing O_2 for 5 h at 823 K and cooled under flowing O_2 to reaction temperature (473–498 K). Details for different pretreatment protocols are explicitly stated in the Figure captions. Upon reaching reaction temperature, the zeolite was purged under 50 mL min^{-1} of He for 0.5 h. The gas flow was then changed to 80 mL min^{-1} CH_4 for 0.5 h followed by 80 mL min^{-1} of CH_4, H_2O, and O_2 (typically 98.1 kPa, 3.2 kPa, and 0.0025 kPa respectively). CH_3OH partial pressures

evolved during catalytic CH_4 oxidation were quantified using a gas chromatograph (Agilent Technologies, model 6890N) equipped with an S-bond column (Restek Rt-S-bond, 30 m, 0.25 mm ID, #19770) and flame ionization detector. The oven temperature was isothermal at 373 K for 30 min.

Simulated high conversion CH_4 oxidation experiments were performed in the same reactor described above. Catalyst activation was the same as described above. Liquid reactants CH_3OH and H_2O were introduced into the gas stream via saturators maintained at 273 K and 298 K respectively. The reaction mixture of 0.70 kPa CH_3OH, 2.25 kPa H_2O, and variable O_2 partial pressure was attained by combining two gas streams at the inlet of the reactor: 1) 15 mL min^{-1} He directed through CH_3OH contained in a saturator, and 2) 65 mL min^{-1} total of 1% O_2 in He and/or He gas streams directed through H_2O contained in a saturator. CH_3OH, dimethyl ether, CO_2, and H_2O were monitored using a gas chromatograph (Agilent Technologies, model 6890N) equipped with thermal conductivity detector and a Carboxen 1006 PLOT column (Sigma-Aldrich, 30 m, 0.32 mm ID, #24241-U). The oven temperature profile was initially 313 K for 2 min, then ramped 10 K min^{-1} to 393 K, and then isothermal for 15 min.

Product quantification. Calibration curves for CH_3OH were constructed using a known vapor pressure of CH_3OH taken into a CH_4 stream. CH_3OH vapor pressure was controlled by immersing the saturator containing CH_3OH into cooling baths at several temperatures (e.g. ice water at 273 K, dry ice in ethanol at 201 K, etc). Relative response factors were calculated using the gas chromatograph between known CH_4 and CH_3OH partial pressures. Calibration curves for CO_2 were constructed by flowing known mixtures of 1% CO_2/helium and helium to a gas chromatograph-mass spectrometer.

The following definitions were used to quantify experimental data:

The large partial pressure of CH_4 in the gas stream during catalytic CH_4 oxidation reactions prevented the accurate quantification of CH_4 consumption. As such, CH_4 conversion was assumed to be equal to the total molar flow rate of carbon of all observed products divided by the initial molar flow rate of CH_4:

$$X_{CH4} = \frac{\sum_{i=1}^{N} C_i F_i}{F_{CH4,0}}$$

where X_{CH4} is the conversion of CH_4, F_i is the molar flow rate of product i, C_i is the number of carbon atoms in product i, $\Sigma\, C_i F_i$ is the total molar flow rate of carbon of all products, and $F_{CH4,0}$ is the initial molar flow rate of CH_4.

As explained above, the amount of CH_4 consumed was not quantifiable. Thus, product selectivity for catalytic CH_4 oxidation was defined as:

$$S_i = \frac{C_i F_i}{\sum_{i=1}^{N} C_i F_i}$$

where S_i is the selectivity of product i, C_i is the number of carbon atoms in product i, F_i is the molar flow rate of product i, and $\Sigma\, C_i F_i$ is the total molar flow rate of carbon of all products.

For CH_3OH oxidation experiments, CH_3OH conversion was defined as:

$$X_{CH3OH} = 1 - \frac{F_{CH3OH}}{F_{CH3OH,0}}$$

where X_{CH3OH} is the conversion of CH_3OH, F_{CH3OH} is the molar flow rate of CH_3OH at steady state, and $F_{CH3OH,0}$ is the initial molar flow rate of CH_3OH.

Product selectivity was defined as:

$$S_i = \frac{C_i F_i}{F_{CH3OH,0} - F_{CH3OH}}$$

where S_i is the product selectivity, C_i is the carbon number for product *i*, F_i is the molar flow rate of product *i*, and $F_{CH3OH,0} - F_{CH3OH}$ is the molar flow rate of CH_3OH reacted at steady state.

Product yield was defined as:

$$Y_i = \frac{C_i F_i}{F_{CH3OH,0}}$$

where Y_i was the yield for product *i*, F_i is the steady state molar flow rate of product *i*, C_i is the number of carbon atoms in product *i*, and $F_{CH3OH,0}$ is the initial molar flow rate of CH_3OH.

Transient experiments with isotopically labelled molecules. The isotopically labeled experiments were performed in the reactor setup described in the introduction to the Catalytic CH_4 oxidation reactions subsection. ^{13}C-methoxy species were deposited on the zeolite surface by exposing a freshly activated zeolite to 50 mL min^{-1} of 17% $^{13}CH_4$/He (using $^{13}CH_4$ [99 atom % ^{13}C, Sigma Aldrich]) for 0.5 h. ^{13}C-methoxy species were extracted with a mixture of $^{12}CH_4/H_2O/O_2$ (98.1/3.2/0.0025 kPa). $^{13}CH_4$ pulses were introduced by flowing a 3.2 kPa H_2O, 0.0025 kPa O_2, and balance $^{13}CH_4$ gas mixture at a flow rate of 10 mL min^{-1} for 0.5 h before resuming a flow of 3.2 kPa H_2O, 0.0025 kPa O_2, and $^{12}CH_4$ balance. CH_3OH and CO_2 isotopes were analyzed using a gas chromatograph (Agilent Technologies, model 7890N) equipped with a quadrupole mass spectrometer and an S-bond column (Restek Rt-S-bond, 30 m, 0.25 mm ID, #19770). The oven temperature profile was isothermal at 373 K for 30 min. $^{13}CO_2$ was tracked with m/z = 45. $^{13}CH_3OH$ was monitored using m/z = 33 instead of 32 because of small O_2 leaks into the gas chromatograph-mass spectrometer. O_2 leaks elevated the m/z = 32 signal and prevented the detection of trace $^{13}CH_3OH$ signals relative to background O_2. However, m/z = 33 did not interfere with O_2.

Section S1: Product Identification for CH_4 Oxidation over Cu-Na-ZSM-5 (Cu/Al = 0.37)

Cu-Na-ZSM-5 was activated under oxygen (O_2) for 5 h at 823 K, cooled to reaction temperature at 483 K under flowing O_2, and then purged under helium (He) for 1 h. After reaction with methane (CH_4) for 0.5 h, an extraction gas of 3.2 kPa of water (H_2O), 0.0025 kPa O_2 and CH_4 balance was flowed over the Cu-Na-ZSM-5 bed. A steady state methanol (CH_3OH) rate of 0.88 μmol h^{-1} g_{cat}^{-1} was achieved after 10 h on-stream (Figure 1). A condenser was placed in-line downstream from the catalyst bed. Next, the gas stream containing $CH_4/H_2O/O_2$ and the oxidation products was passed through the condenser maintained at 201 K in a dry ice-ethanol bath. After 6 h on-stream, the frozen products were thawed in D_2O, removed from the in-line condenser, and injected into a quartz nuclear magnetic resonance (NMR) tube (528-PP-7, Wilmad LabGlass) for analysis. ^{1}H-NMR performed on the condensate in a 500 MHz spectrometer (Varian Inova-500) showed CH_3OH as the only product (Figure S1). Gas phase products of the reactor effluent were analyzed using a gas chromatograph equipped with a quadrupole mass spectrometer (Agilent 7890N). The only gas phase product from the reaction was carbon dioxide (CO_2). Assuming CO_2 and CH_3OH were the only reaction products, the steady state CH_4 conversion was 0.0014% and the CH_3OH selectivity was 70.6% (Figure S2).

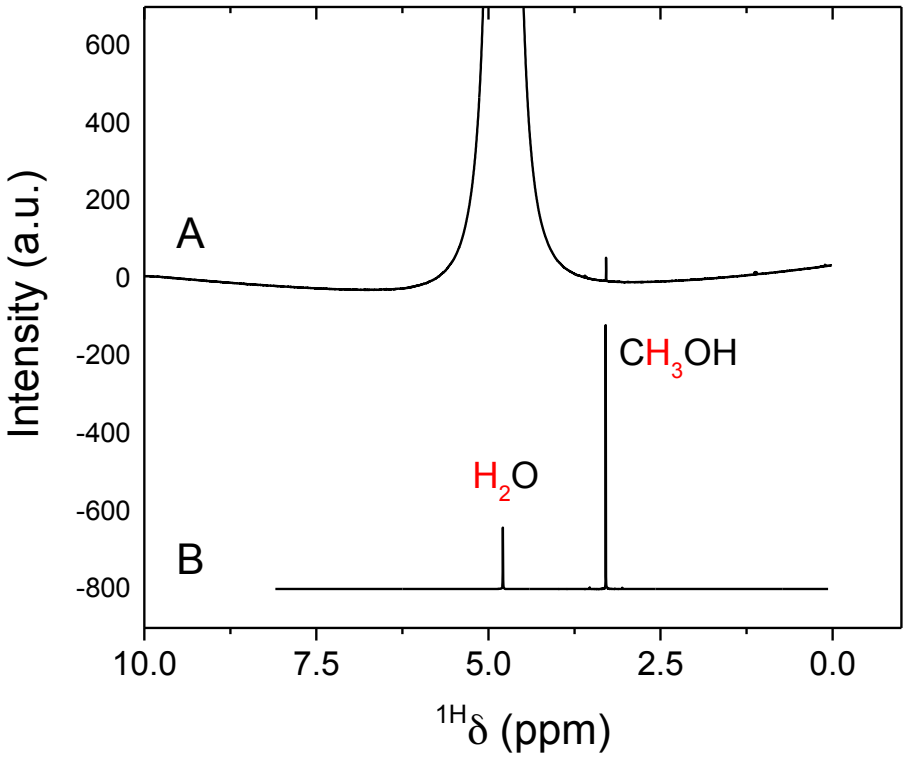

Figure S1. ^{1}H-NMR spectrum of liquid oxygenated products from CH_4 oxidation over Cu-Na-ZSM-5 (Cu/Al = 0.37) collected in a dry ice/ethanol cold trap.
(A) ^{1}H-NMR of liquid products from steady state CH_4 oxidation over Cu-Na-ZSM-5 (Cu/Al = 0.37, Na/Al = 0.26) condensed in a condenser immersed in a dry ice-ethanol bath after 6 h on-stream. **(B)** ^{1}H-NMR of a CH_3OH standard in D_2O.

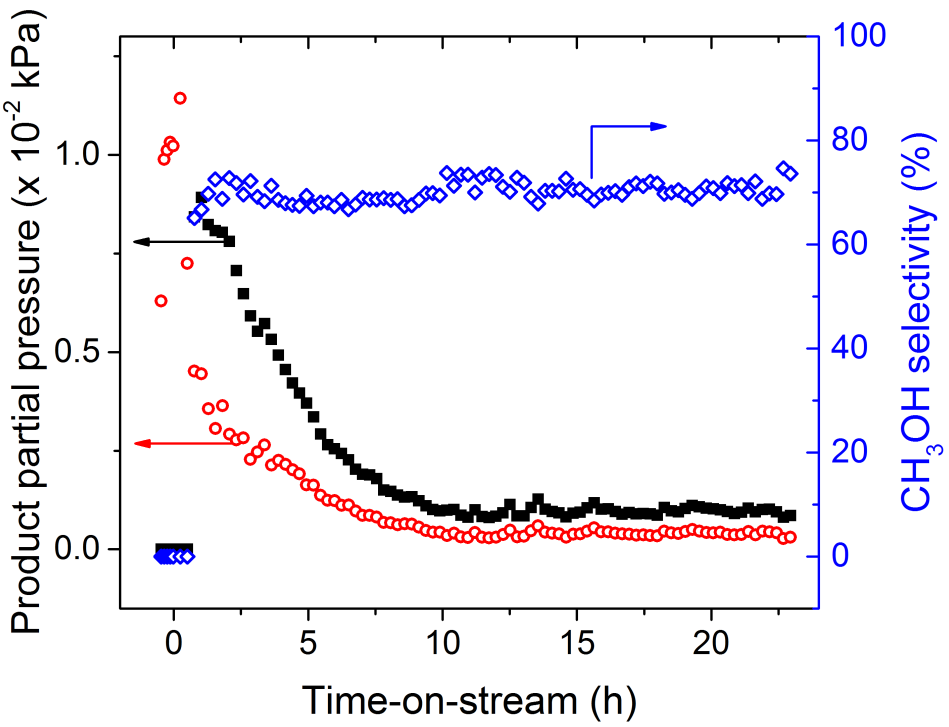

Figure S2. Selectivity and product partial pressures for CH_4 oxidation over Cu-Na-ZSM-5 (Cu/Al = 0.37, Na/Al = 0.26).

Catalyst pretreatment: 5 h at 823 K under flowing O_2,, cooled to 483 K under O_2 flow and then purged under He for 0.5 h. Initial CH_4 oxidation: 0.5 h under 2400 mL h^{-1} g_{cat}^{-1} of CH_4 at 483 K. Reaction conditions: T = 483 K, WHSV = 2400 mL h^{-1} g_{cat}^{-1}, P_{CH4} = 98.1 kPa, P_{H2O} = 3.2 kPa, P_{O2} = 0.0025 kPa (25 ppm). (▪) CH_3OH partial pressure (kPa). (○) CO_2 partial pressure (kPa). (◊) CH_3OH selectivity

Section S2: Simulation of High Conversion CH_4 Oxidation via CH_3OH Oxidation over Cu-Na-ZSM-5 (Cu/Al = 0.37)

The over-oxidation of CH_3OH into CO_2 at higher CH_4 conversion levels was simulated by introducing CH_3OH as a reactant. The direct oxidation of CH_4 into CH_3OH over copper-exchanged ZSM-5 under regular conditions generated a conversion of 0.0014 %. At these conditions, the low O_2 partial pressure (0.0025 kPa) was sufficient to convert CH_4 into CH_3OH (4.5×10^{-4} kPa O_2 is needed to produce CH_3OH at a rate of 0.88 μmol h^{-1} g_{cat}^{-1}), but it was observed that the excess O_2 further oxidized CH_3OH into CO_2 at 483 K (30% selectivity to CO_2). Therefore, since higher conversion of CH_4 (e.g. 1%) will require more O_2 in the reaction mixture, the excess O_2 at this scale could also over-oxidize CH_3OH into CO_2 decreasing the overall selectivity of the process.

To evaluate CO_2 selectivity at higher CH_4 conversions, CH_3OH was used as a reactant to simulate the gas composition the Cu-Na-ZSM-5 (Cu/Al = 0.37) catalyst bed would encounter at 100% CH_4 conversion. After activating Cu-Na-ZSM-5 for 5 h at 823 K under O_2, the zeolite bed was cooled to 483 K and purged under He for 1 h. Then a reaction mixture of 0.70 kPa CH_3OH, variable O_2 partial pressure, 2.25 kPa H_2O and He was passed over the catalyst bed. Flowing this reaction mixture over Cu-Na-ZSM-5 and measuring the extent of CO_2 production can be used as a surrogate to calculate the maximum CO_2 selectivity. A 0.70 kPa partial pressure of CH_3OH simulated a CH_4 partial pressure of 0.70 kPa being fully converted into CH_3OH. The O_2 partial pressure was varied to represent unreacted or excess O_2 from a typical CH_4 oxidation experiment. Helium (He) was used instead of CH_4 in the gas mixture to isolate CH_3OH oxidation and exclude the coadsorption of CH_4 on the zeolite surface. The gas mixture composed of 0.70 kPa CH_3OH, 2.25 kPa H_2O, and O_2 was flowed over the Cu-Na-ZSM-5 catalyst for 5 h at 483 K before the steady state gas composition was analyzed in order to allow for changes in copper speciation that occur in regular CH_4 oxidation experiments (Figure 3 – S11). As the O_2 partial pressure was increased from 0.21 kPa to 2.70 kPa, the CO_2 yield increased from 6.8% to 24% (Figure S3A). The rate order of O_2 in CH_3OH oxidation was ca. 0.50 (Figure S3B). As expected, lower amounts of O_2 relative to CH_3OH (lower O_2/CH_3OH partial pressure ratio) suppress the formation of CO_2. However, even having up to 4 times the partial pressure of O_2 as CH_3OH only generated a 24% yield and 25% selectivity of CO_2, which was a lower CO_2 selectivity than that observed during regular CH_4 oxidation experiments over Cu-Na-ZSM-5 at similar conditions (Figure S2, $P_{O2}/P_{CH3OH} = 2.5$). Therefore, these results suggest that CH_4 oxidation to higher conversions will not result in a substantial increase in CO_2 production or a decrease in CH_3OH selectivity at 483 K.

CO_2 selectivity could be further reduced by lowering the temperature of the simulated gas mixture over Cu-Na-ZSM-5. As the reaction temperature was lowered to 463 K, the CO_2 yield and selectivity decreased from 24% to 7.4% (Figure S4). These data show that CH_3OH selectivity could increase beyond 70% by lowering the reaction temperature (< 483 K) in a high conversion CH_4 oxidation process.

CH_3OH conversion was greater than 90% for the simulated, high conversion CH_4 oxidation experiments (Figure S3A) where the vast majority of CH_3OH was converted into dimethyl ether (DME) (> 60% yield). DME is produced from the acid-catalyzed dehydration of CH_3OH.[4] Brønsted acid sites in zeolites are well known to perform this reaction between 473 and 573 K.[5,6] However, zeolites can still produce DME even with trace Bronsted acidity,[7] such as that present in sodium-exchanged ZSM-5.[8] CH_3OH dehydration is thermodynamically favorable under the CH_3OH oxidation reaction conditions of 483 K, 0.70 kPa CH_3OH, and 2.25 kPa H_2O. The

reaction 2 $CH_3OH \leftrightarrow (CH_3)_2O + H_2O$ has a chemical equilibrium constant (K_{eq}) of 14.8 under these reaction conditions, and the equilibrium conversion of CH_3OH to DME would be 92%.

In the simulated, high conversion CH_4 oxidation experiments, the DME yield decreased from 80% to 62% as the O_2 partial pressure increased from 0.21 kPa to 2.7 kPa (Figure S3A), consistent with CH_3OH or DME being oxidized into CO_2. At a lower temperature of 463 K, the DME yield increased from 62% to 74% (Figure S4).

DME was not observed in typical CH_4 oxidation experiments over Cu-Na-ZSM-5 due to the low equilibrium conversion of CH_3OH into DME. At steady state, taking the CH_3OH partial pressure to be 10^{-3} kPa and the H_2O partial pressure to be 3.2 kPa, the equilibrium conversion of CH_3OH into DME at 483 K would be 0.90%. The theoretical maximum amount of DME that could be produced was below the detection limit of the gas chromatograph used to quantify steady state rates.

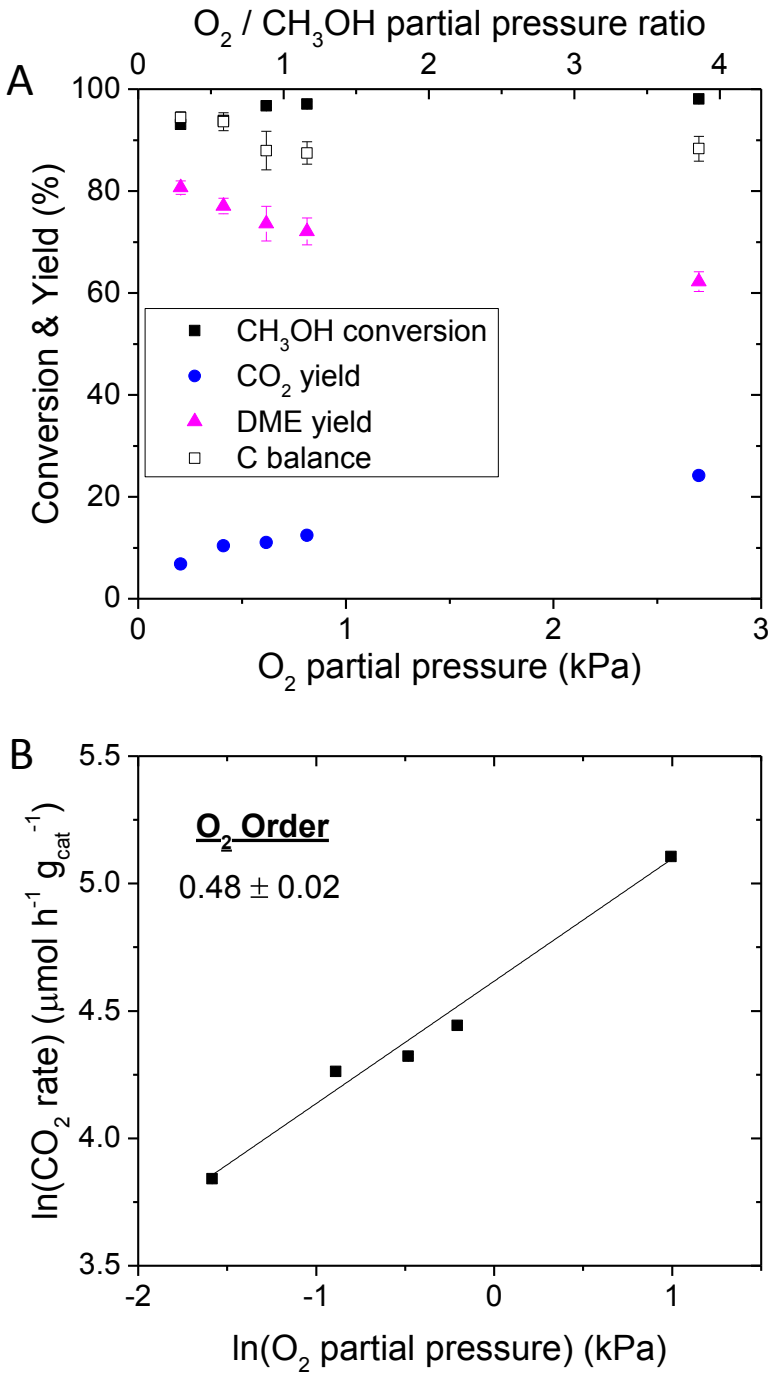

Figure S3. Simulation of high conversion CH_4 oxidation over Cu-Na-ZSM-5 versus O_2 partial pressure.

(A) CH_3OH oxidation as a function of O_2 partial pressure and **(B)** order of O_2 for CH_3OH oxidation over Cu-Na-ZSM-5 (Cu/Al = 0.37, Na/Al = 0.26). **(A)** Pretreatment: 5 h at 823 K under O_2, cooled under O_2 flow to 483 K and then purged 0.5 h under He. Reaction conditions: T = 483 K, WHSV = 2400 mL h^{-1} g_{cat}^{-1}, P_{CH3OH} = 0.70 kPa, P_{H2O} = 2.25 kPa, He balance. **(B)** Same conditions as **(A)**. Error bars and ± denote 95% confidence intervals.

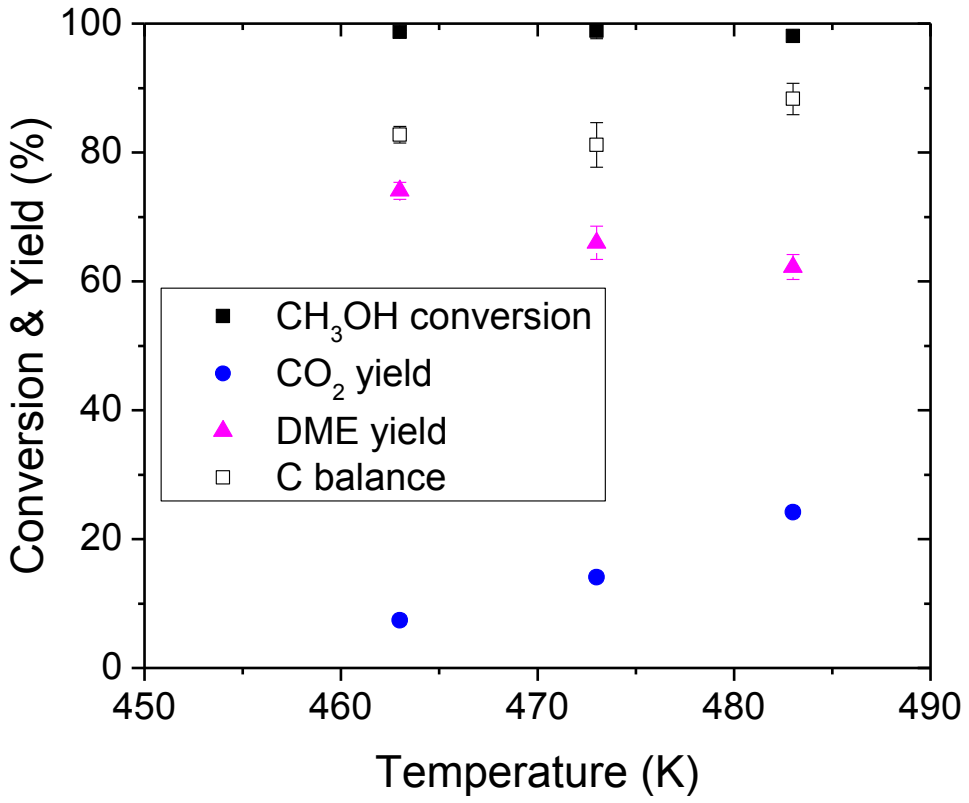

Figure S4. Simulation of high conversion CH_4 oxidation over Cu-Na-ZSM-5 versus reaction temperature.
Pretreatment: 5 h at 823 K under O_2, cooled under O_2 flow to 483 K and purged 0.5 h under He Reaction conditions: WHSV = 2400 mL h^{-1} g_{cat}^{-1}, P_{CH3OH} = 0.70 kPa, P_{H2O} = 2.25 kPa, P_{O2} = 2.70 kPa, He balance. Error bars denote 95% confidence intervals.

Section S3: Steady-state CH_3OH Production over Cu-H-ZSM-5 (Cu/Al = 0.31)

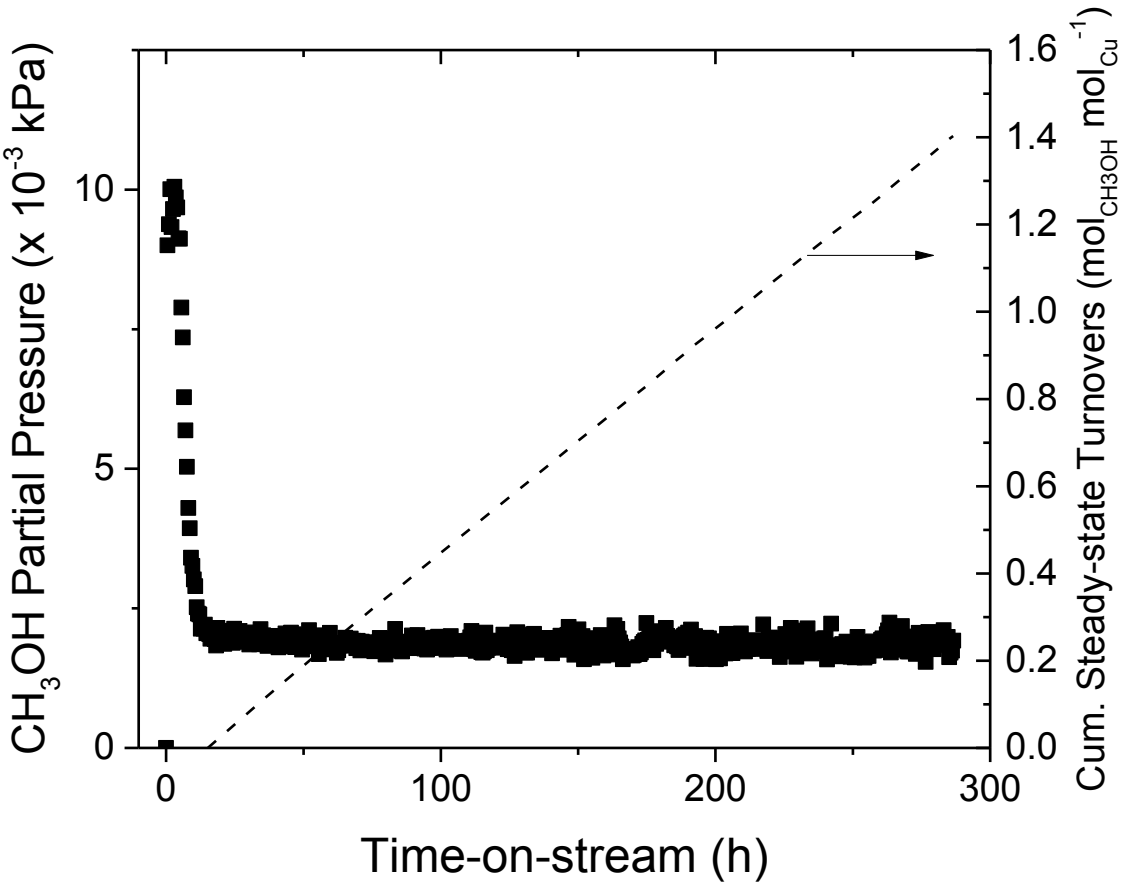

Figure S5. CH_4 oxidation over Cu-H-ZSM-5 (Cu/Al = 0.31).
Catalyst pretreatment: 5 h at 823 K under flowing $O_{2,}$, cooled to 483 K under O_2 flow and then purged under He for 0.5 h. Initial CH_4 oxidation: 0.5 h under 2400 mL h^{-1} g_{cat}^{-1} of CH_4 at 483 K. Reaction conditions: T = 483 K, WHSV = 2400 mL h^{-1} g_{cat}^{-1}, P_{CH4} = 98.1 kPa, P_{H2O} = 3.2 kPa, P_{O2} = 0.0025 kPa (25 ppm). Dashed line denotes cumulative turnovers collected at steady-state.

Section S4: ^{13}C Isotopically Labelled Control Experiments over Cu-Na-ZSM-5 (Cu/Al = 0.37)

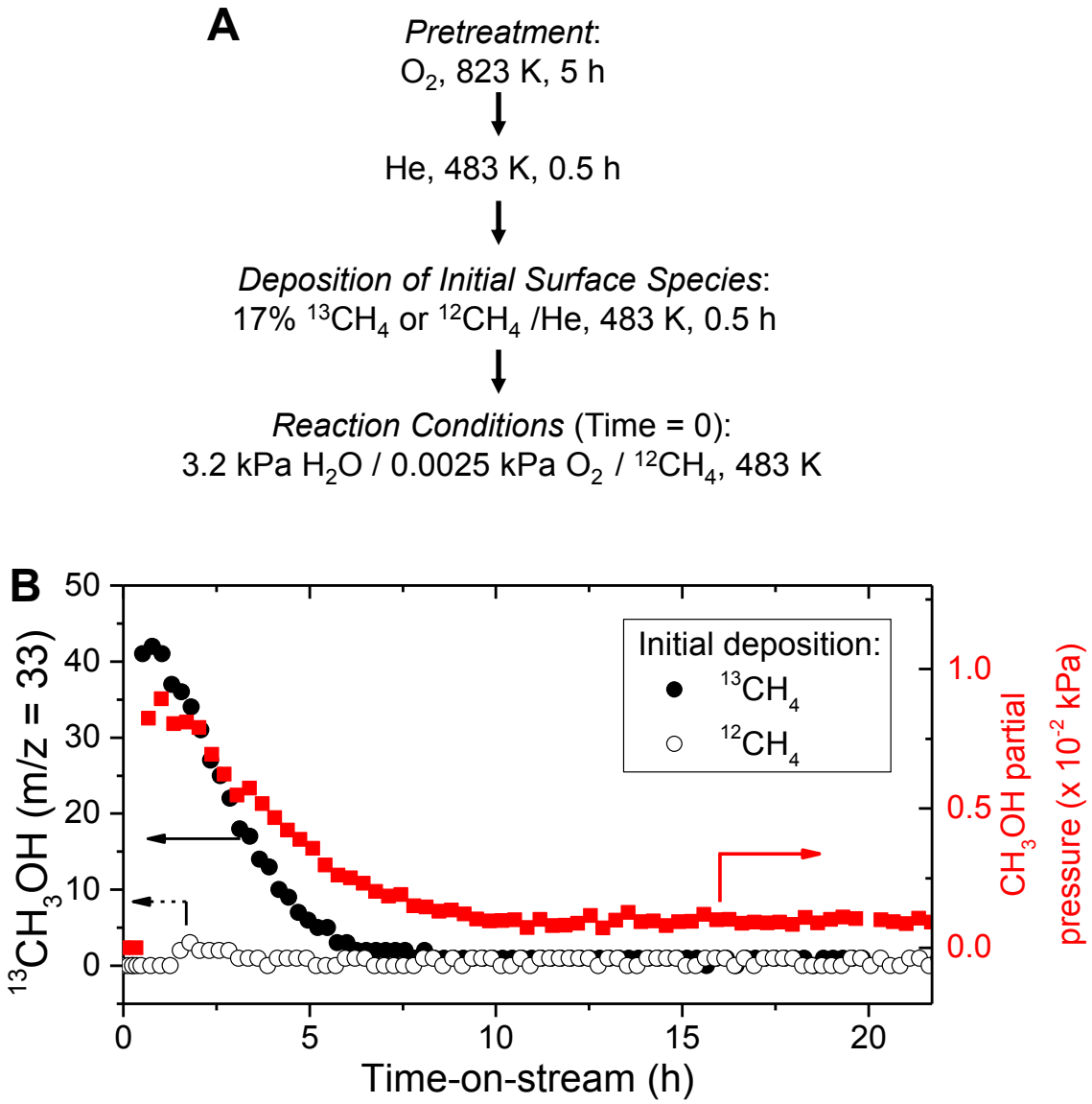

Figure S6. Isotopically labeled kinetic experiments over Cu-Na-ZSM-5 (Cu/Al = 0.37, Na/Al = 0.26).
(A) Experimental pretreatment protocols used for the initial deposition of surface species on Cu-Na-ZSM-5 with $^{13}CH_4$ or $^{12}CH_4$. **(B)** Extraction of CH_3OH from the Cu-Na-ZSM-5 surface initially deposited by $^{13}CH_4$ (●) or $^{12}CH_4$ (○). Reaction conditions: T = 483 K, WHSV = 2400 mL h^{-1} g_{cat}^{-1}, P_{12CH4} = 98.1 kPa, P_{H2O} = 3.2 kPa, P_{O2} = 0.0025 kPa (25 ppm).

Section S5: $^{13}CO_2$ Production during Transient, Isotopically Labelled Experiments over Cu-Na-ZSM-5 (Cu/Al = 0.37)

^{13}C methoxy species were deposited on the zeolite by flowing $^{13}CH_4$ (16.8 kPa $^{13}CH_4$ [99 atom% ^{13}C, Sigma-Aldrich] with balance He) over activated Cu-Na-ZSM-5 for 0.5 h at 483 K and then using a regular $^{12}CH_4/H_2O/O_2$ gas mixture to evolve oxidation products from the zeolite. As shown in Figure S7A, enriched $^{13}CO_2$ (m/z = 45) is quickly produced in the stoichiometric regime, but unlabeled $^{12}CO_2$ is observed in the steady state regime, thus suggesting unlabeled ^{12}C surface species are oxidized into $^{12}CO_2$ once the ^{13}C species are depleted. The reaction rate remained at steady state (rate = 0.88 μmol_{CH3OH} h^{-1} g_{cat}^{-1}) for 21 h at a weight hourly space velocity (WHSV) of 2400 mL h^{-1} g_{cat}^{-1} (equivalent to the production of 18.5 µmol g_{cat}^{-1} of $^{12}CH_3OH$). Next, the gas mixture was switched to $^{13}CH_4/H_2O/O_2$ for 0.5 h at a WHSV = 300 mL h^{-1} g_{cat}^{-1} before resuming the flow of the regular, unlabeled mixture. This $^{13}CH_4$ pulse resulted in the production of $^{13}CO_2$ during steady state CH_3OH production as evidenced by the pulse of m/z = 45 signal in Figure S7A. Control experiments using $^{12}CH_4$ to populate the activated catalyst with unlabeled ^{12}C methoxy species did not generate a significant amount of $^{13}CO_2$ in the stoichiometric or steady state regimes (Figure S7C).

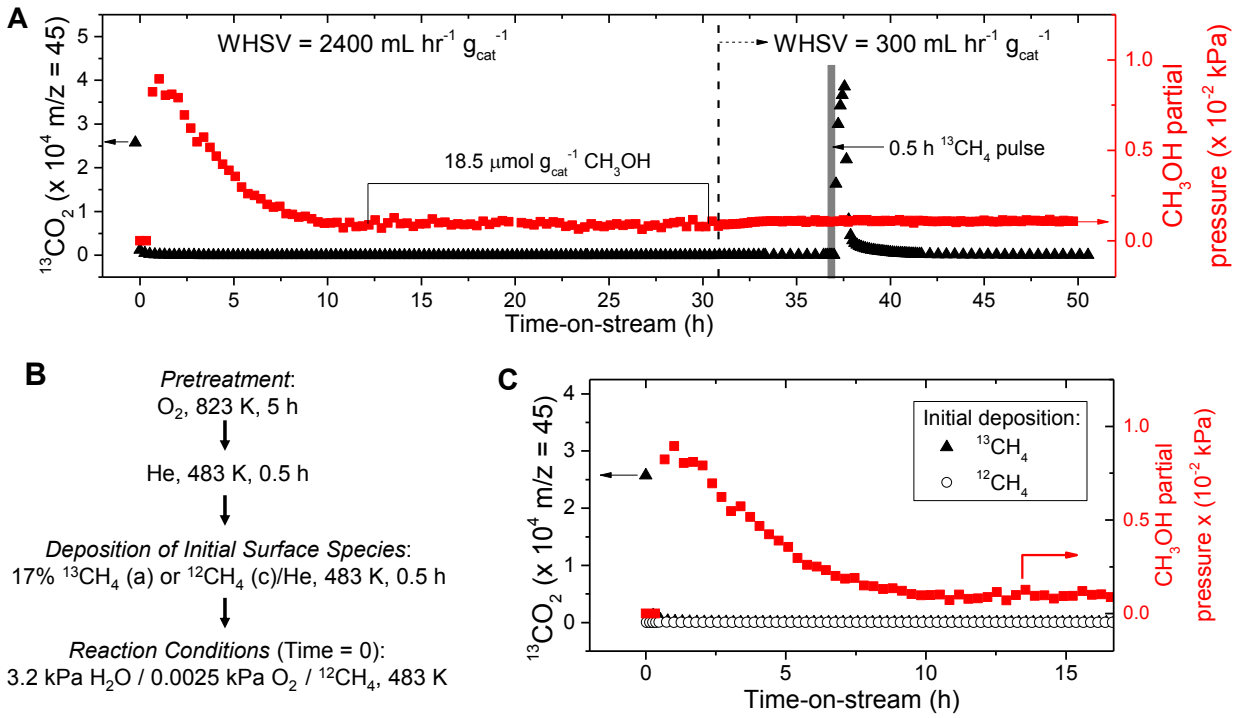

Figure S7. Transient, isotopically labeled kinetic experiments over Cu-Na-ZSM-5 (Cu/Al = 0.37, Na/Al = 0.26).

(A) $^{13}CO_2$ production from initial deposition of $^{13}CH_4$ on Cu-Na-ZSM-5 surface and transient, pulsed $^{13}CH_4$. **(B)** Experimental pretreatments for panels **(A)** and **(C)**. **(C)** Comparison of $^{13}CO_2$ production using $^{13}CH_4$ or $^{12}CH_4$ after activation of Cu-Na-ZSM-5.

(A) Reaction conditions: T = 483 K, WHSV = 2400 mL h^{-1} g_{cat}^{-1}, P_{12CH4} = 98.1 kPa, P_{H2O} = 3.2 kPa, P_{O2} = 0.0025 kPa (25 ppm). After 31 h on-stream, WHSV was reduced to 300 mL h^{-1} g_{cat}^{-1}. Gray area denotes 0.5 h pulse of P_{13CH4} = 98 kPa, P_{H2O} = 3.2 kPa, P_{O2} = 0.0025 kPa. (▲) $^{13}CO_2$ evolution and (■) CH_3OH partial pressure (kPa). **(C)** Reaction conditions: T = 483 K, WHSV =

2400 mL h^{-1} g_{cat}^{-1}, P_{12CH4} = 98.1 kPa, P_{H2O} = 3.2 kPa, P_{O2} = 0.0025 kPa. Initial deposition of surface species used either 17% $^{13}CH_4$ (▲) or $^{12}CH_4$ (○) in He at 483 K.

Section S6: Isotopically Labelled Experiments over Cu-H-ZSM-5 (Cu/Al = 0.31)

Catalytic turnover was also verified over Cu-H-ZSM-5 (Cu/Al = 0.31) using similar experimental procedures as outlined in Figure S6A. When an activated Cu-H-ZSM-5 was reacted with $^{13}CH_4$ before extraction (Figure S8A), a large pulse of $^{13}CH_3OH$ was observed in the stoichiometric regime. However, as CH_3OH production approached steady state, $^{13}CH_3OH$ production declined and resulted in the production of exclusively $^{12}CH_3OH$ (Figure S8B). However, virtually no $^{13}CH_3OH$ was extracted from the zeolite when $^{12}CH_4$ was used for the initial reaction. These experiments show that the source carbon for CH_3OH produced at steady state must come from gas phase $^{12}CH_4$, thereby indicating turnover on the Cu-H-ZSM-5 surface.

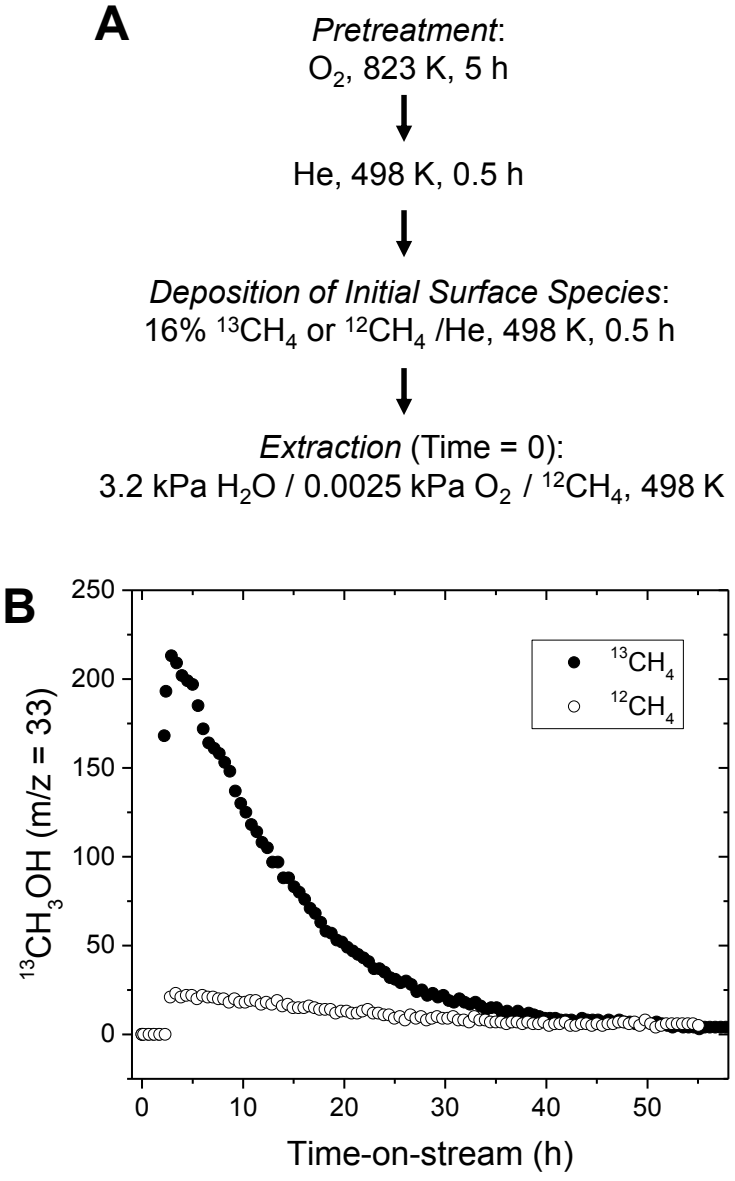

Figure S8. Isotopically labeled studies over Cu-H-ZSM-5 (Cu/Al = 0.31).
(A) Experimental pretreatments for panel **(B)**. **(B)** Extraction of $^{13}CH_3OH$ from Cu-H-ZSM-5 surface initially deposited by $^{13}CH_4$ (●) or $^{12}CH_4$ (○). Reaction conditions: T = 498 K, WHSV = 300 mL h^{-1} g_{cat}^{-1}, P_{12CH4} = 98.1 kPa, P_{H2O} = 3.2 kPa, P_{O2} = 0.0025 kPa (25 ppm).

Section S7: Kinetic Order Dependence of Reactants and Transient, Isotopic Pulsing of CD_4 over Cu-Na-ZSM-5 (Cu/Al = 0.37)

The partial pressure of O_2 was varied over Cu-Na-ZSM-5 (Cu/Al = 0.37, Na/Al = 0.26) to deduce the order of O_2 on catalytic CH_4 oxidation activity. After activating the zeolite under O_2 at 823 K for 5 h, Cu-Na-ZSM-5 was cooled to 483 K under O_2 flow, purged under He, and reacted under dry 75% CH_4/He at 483 K for 0.5 h. Afterwards, 3.2 kPa H_2O and O_2 were then introduced into the reactant stream. The O_2 partial pressure was controlled using a 1% O_2/N_2 gas stream co-fed with He while maintaining CH_4 and H_2O partial pressures at 72.5 kPa and 3.2 kPa respectively. As the partial pressure of O_2 decreased, the observed catalytic CH_3OH production rate remained fairly constant, showing the rate was zero order with respect to O_2 (Figure S9A).

The catalytic CH_3OH production rate demonstrated positive kinetic orders with respect to CH_4 and H_2O partial pressures. The rate dependence of CH_4 was investigated by varying CH_4 partial pressure from 49 to 98 kPa while maintaining H_2O and O_2 partial pressures constant at 3.2 kPa and 0.0025 kPa respectively. The catalytic rate of CH_3OH production exhibited a first order dependence on CH_4 partial pressure (Figure S9B), indicating the dilution of CH_4 in the reaction feed is undesired. Similarly, H_2O increased the production of CH_3OH from Cu-Na-ZSM-5. H_2O vapor pressure was controlled between 1.1 to 3.2 kPa using aqueous $CaCl_2$ solutions in a saturator maintained at 298 K. The CH_4 and O_2 partial pressures were kept constant at 98 and 0.0025 kPa respectively. CH_3OH production decreased as the H_2O partial pressure decreased (Figure S9C) by order of 0.5. As expected, when no H_2O was delivered to the catalyst, no CH_3OH was detected, indicating that H_2O was necessary for CH_3OH extraction.

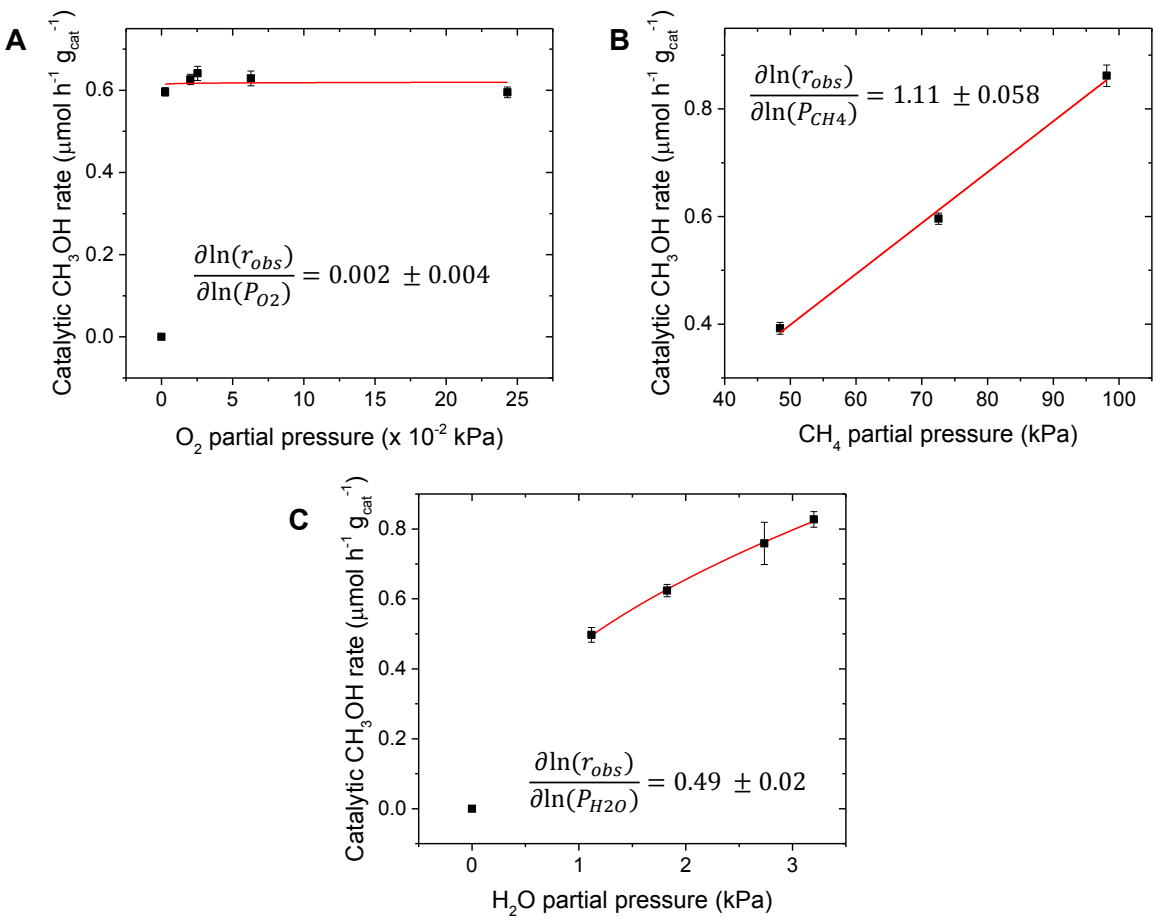

Figure S9. Kinetic order of reactants for catalytic CH_4 oxidation over Cu-Na-ZSM-5 (Cu/Al = 0.37)

The effect of **(A)** O_2 partial pressure, **(B)** CH_4 partial pressure, and **(C)** H_2O partial pressure on CH_4 oxidation over Cu-Na-ZSM-5. Catalyst pretreatment: 5 h at 823 K under flowing O_2,, cooled to 483 K under O_2 flow and then purged under He for 0.5 h. Initial CH_4 oxidation: 0.5 h under 2400 mL h^{-1} g_{cat}^{-1} CH_4.

Reaction conditions: **(A)** T = 483 K, WHSV = 2400 mL h^{-1} g_{cat}^{-1}, P_{CH4} = 72.5 kPa, P_{H2O} = 3.2 kPa, He balance. **(B)** T = 483 K, WHSV = 2400 mL h^{-1} g_{cat}^{-1}, P_{H2O} = 3.2 kPa, P_{O2} = 0.0025 kPa (25 ppm), P_{He} balance. **(C)** T = 483 K, WHSV = 2400 mL h^{-1} g_{cat}^{-1}, P_{CH4} = 98.1 kPa, P_{O2} = 0.0025 kPa (25 ppm), P_{H2O} controlled via saturator filled with aqueous $CaCl_2$ solutions, P_{He} = balance. Error bars and ± denote 95% confidence intervals.

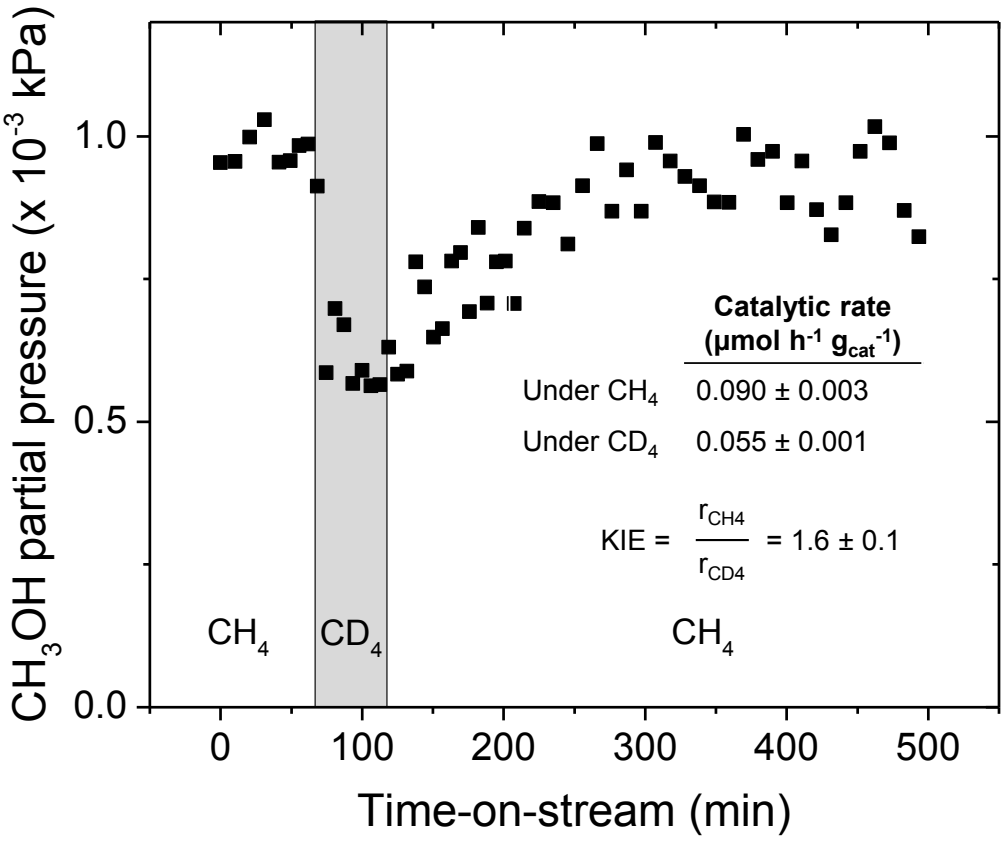

Figure S10. Transient, isotopically labeled CD_4 pulse over Cu-Na-ZSM-5 (Cu/Al = 0.37, Na/Al = 0.26).

Catalyst pretreatment: 5 h at 823 K under flowing O_2,, cooled to 483 K under O_2 flow and then purged under He for 0.5 h. Initial CH_4 oxidation: 0.5 h under 240 mL h^{-1} g_{cat}^{-1} CH_4. Reaction conditions: T = 483 K, WHSV = 240 mL h^{-1} g_{cat}^{-1}, P_{CH4} = 98.1 kPa, P_{H2O} = 3.2 kPa, P_{O2} = 0.0025 kPa (25 ppm). Gray area denotes 0.75 h pulse of CD_4: WHSV = 240 mL h^{-1} g_{cat}^{-1}, P_{CD4} = 98.1 kPa, P_{H2O} = 3.2 kPa, P_{O2} = 0.0025 kPa (25 ppm). KIE = kinetic isotope effect. r_{CH4} = catalytic CH_3OH production rate under CH_4. r_{CD4} = catalytic CH_3OH production rate under CD_4. ± denotes 95% confidence interval.

Section S8: Thermal Pretreatments and the Onset of Catalytic Activity over Cu-Na-ZSM-5 (Cu/Al = 0.37)

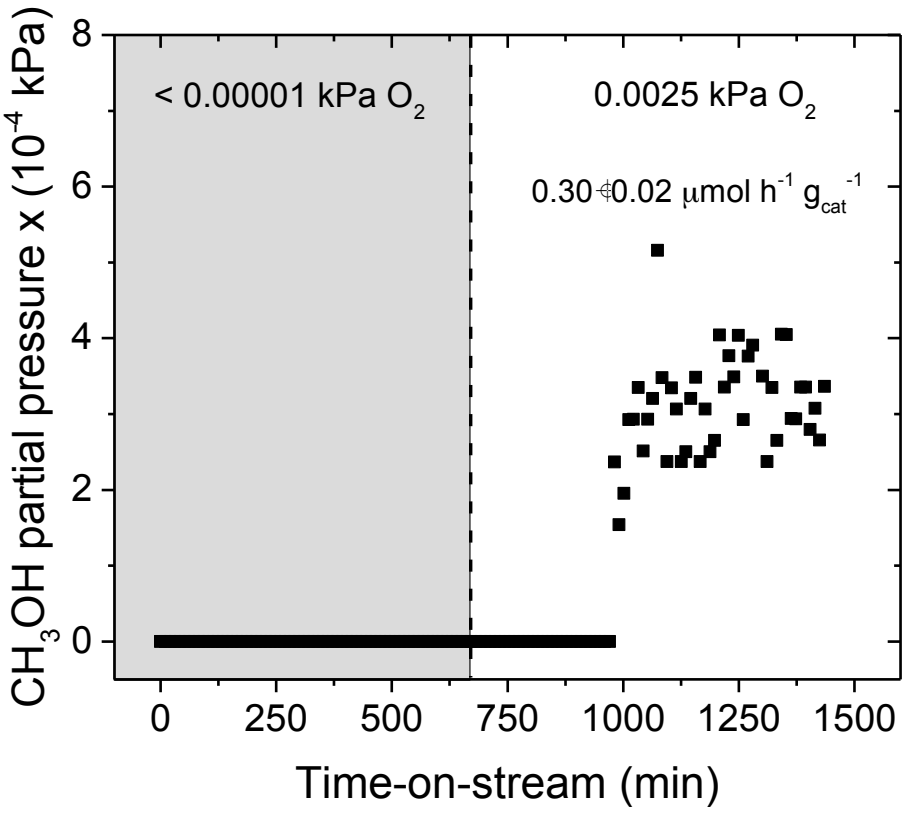

Figure S11. CH_4 oxidation over Cu-Na-ZSM-5 (Cu/Al = 0.37, Na/Al = 0.26) pretreated under O_2-free conditions.
Catalyst pretreatment: 5 h at 823 K under He (< 0.00001 kPa O_2), cooled to 483 K under He flow. Initial CH_4 oxidation: 0.5 h under 2400 mL h^{-1} g_{cat}^{-1} CH_4. Reaction conditions: T = 483 K, WHSV = 2400 mL h^{-1} g_{cat}^{-1}, P_{CH4} = 98.1 kPa, P_{H2O} = 3.2 kPa. Background colors: Gray: P_{O2} = < 0.00001 kPa (0.1 ppm), White: P_{O2} = 0.0025 kPa (25 ppm). O_2 levels reduced to < 0.00001 kPa using a CuO trap. ± denotes 95% confidence interval.

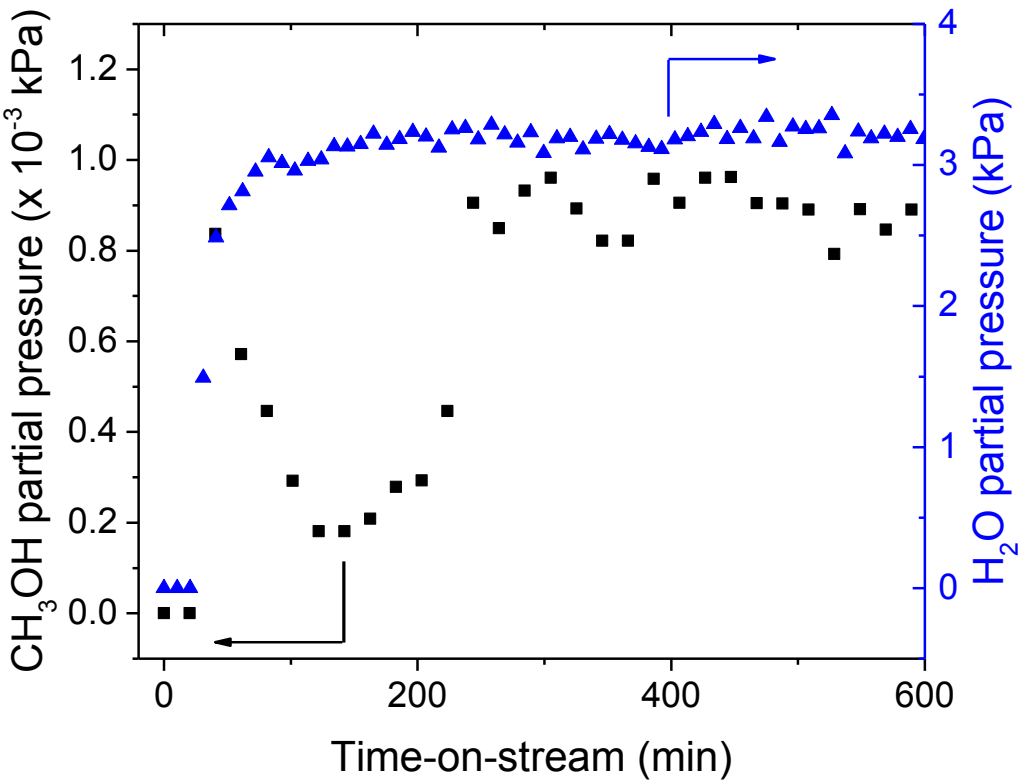

Figure S12. H_2O breakthrough over Cu-Na-ZSM-5 (Cu/Al = 0.37, Na/Al = 0.26) during CH_4 oxidation.
(■) CH_3OH partial pressure (kPa). (▲) H_2O partial pressure (kPa). Pretreatment: ramped under O_2, 5 h at 823 K under He (20 ppm O_2), cooled to 483 K under He. Initial CH_4 oxidation: 0.5 h under 2400 mL h^{-1} g_{cat}^{-1} CH_4. Reaction conditions: T = 483 K, WHSV = 2400 mL h^{-1} g_{cat}^{-1}, P_{CH4} = 98.1 kPa, P_{H2O} = 3.2 kPa, P_{O2} = 0.0025 kPa (25 ppm)

Section S9: In-situ Diffuse Reflectance UV-visible Spectroscopy and Online Gas Chromatography Measurements over Cu-Na-ZSM-5 (Cu/Al = 0.37)

UV-visible spectroscopic and online gas chromatographic measurements were performed over Cu-Na-ZSM-5 (Cu/Al=0.37) to gain insight into copper speciation during pretreatments and steady-state operation. The zeolite was heated at 5 K/min under flowing O_2 to 823 K and then calcined under He (20 ppm O_2) at 823 K for 2 h. A shoulder at 22,700 cm^{-1} decayed within 1 h of He treatment (Figure S13), indicating the majority of the mono-(μ-oxo) dicupric cores were eliminated. Cu-Na-ZSM-5 was then cooled to 483 K under He and then exposed to pure CH_4 for 0.5 h. No significant changes in the UV-visible spectra were observed (Figure S14), further suggesting the elimination of most of the mono-(μ-oxo) dicupric cores. After flowing 93.2 kPa CH_4, 0.051 kPa O_2, and 3.2 kPa H_2O at 483 K, a small amount of stoichiometric CH_3OH was extracted from zeolite before steady-state CH_3OH production (Figure S15A), consistent with kinetic experiments (Figure 3, red symbols). During stoichiometric CH_3OH production, there were no changes in the 22,700 cm^{-1} region (Figure S15B.1-2). Lastly, no bands were present at 22,700 cm^{-1} peak during steady-state CH_3OH production (Figure S15C.1-2, D.1-2), indicating the mono-(μ-oxo) dicupric cores are likely not present during catalytic operation.

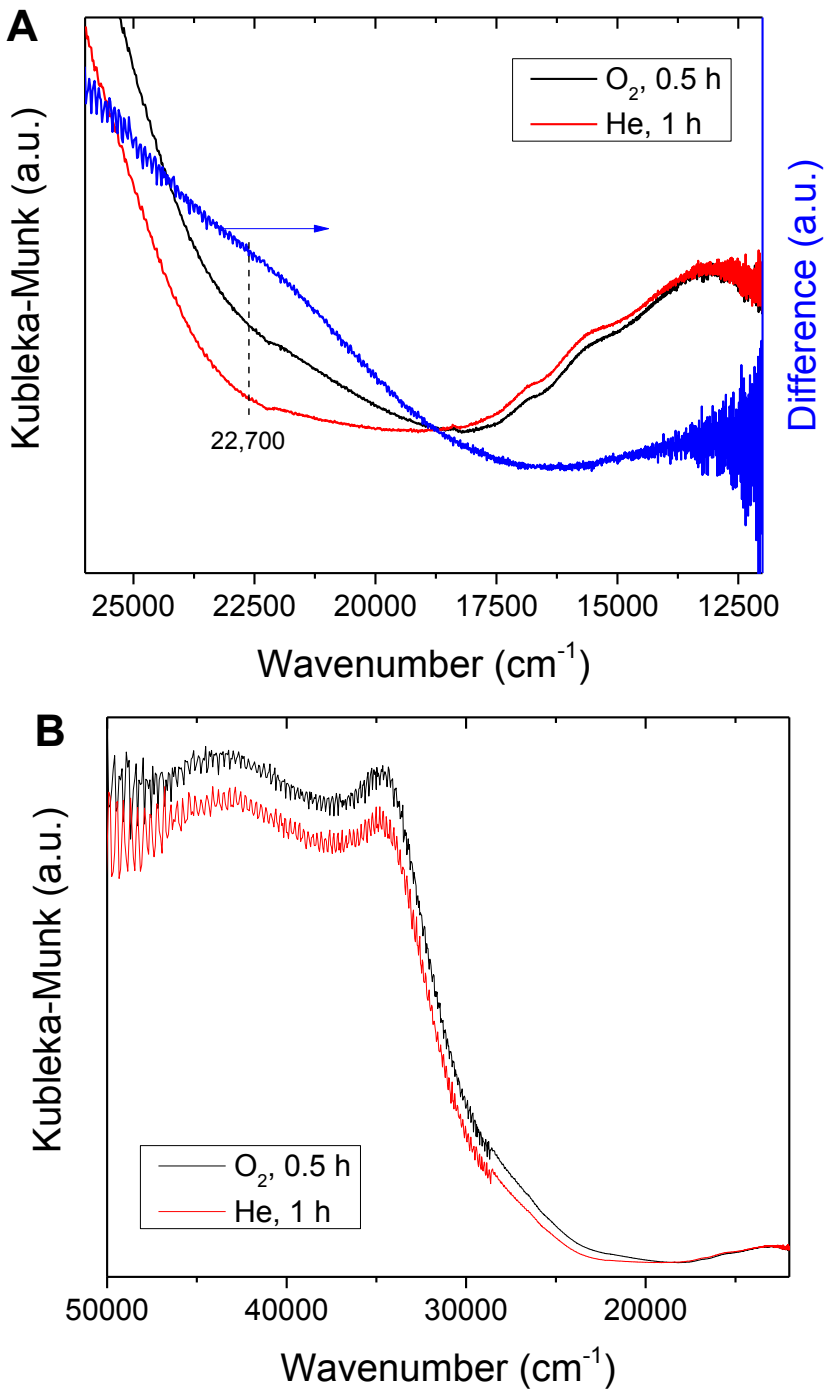

Figure S13. In-situ diffuse reflectance UV-visible spectra of Cu-Na-ZSM-5 (Cu/Al = 0.37) in the (A) visible region and (B) full region. Cu-Na-ZSM-5 was heated under flowing O_2 (5 K/min) to 823 K and held for 0.5 h (black) and then calcined under He (20 ppm O_2) for 2 h (red). Difference spectra (calcined in O_2─calcined in He) are shown (blue, right axis). The decay of the 22,700 cm^{-1} band after He treatment is highlighted.

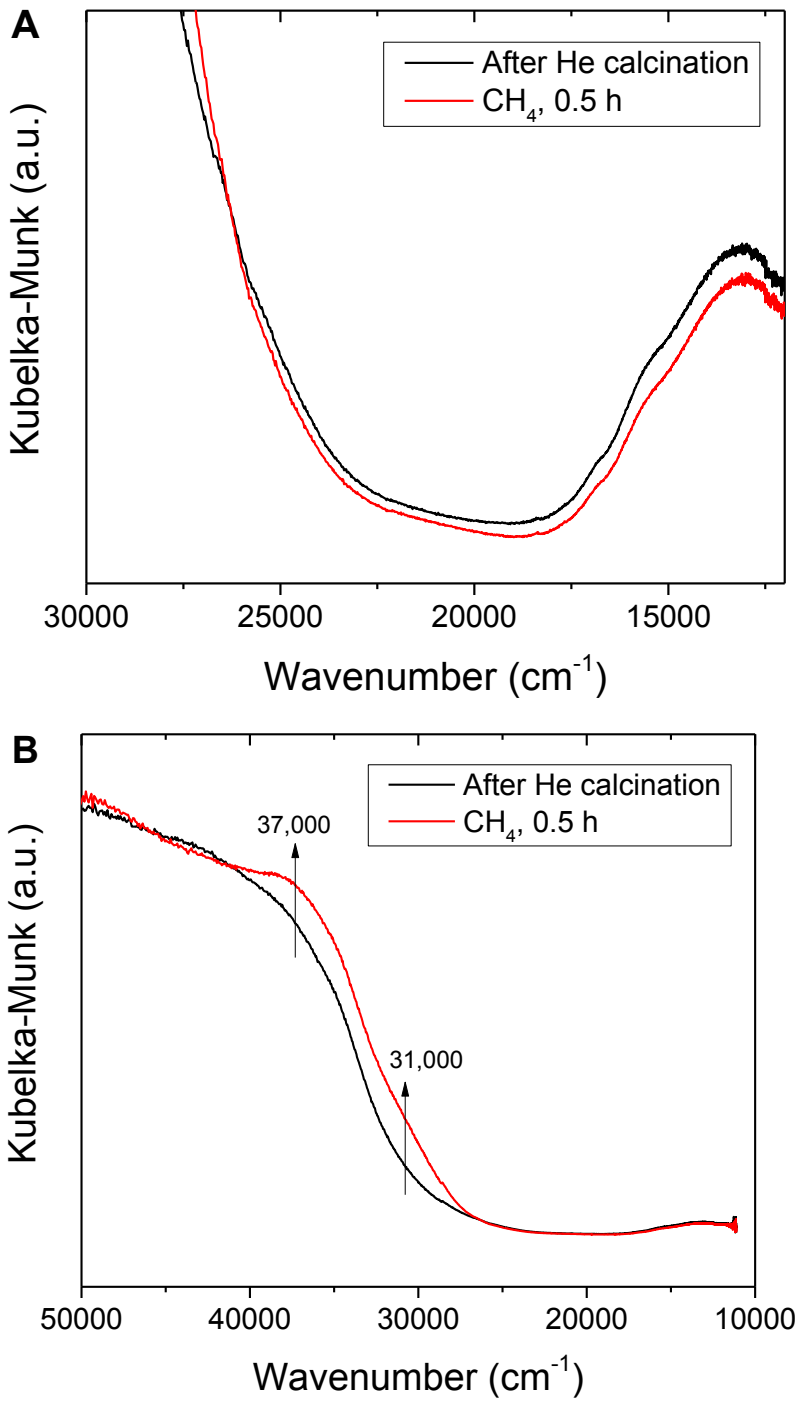

Figure S14. In-situ diffuse reflectance UV-visible spectra of Cu-Na-ZSM-5 (Cu/Al = 0.37) in the (A) visible region and (B) full spectra Catalyst pretreatment: heated to 823 K under flowing O_2, calcined 2 h at 823 K under He (20 ppm O_2) and cooled to 483 K under He. The zeolite was then exposed to CH_4 for 0.5 h. No significant differences were observed in the visible region.

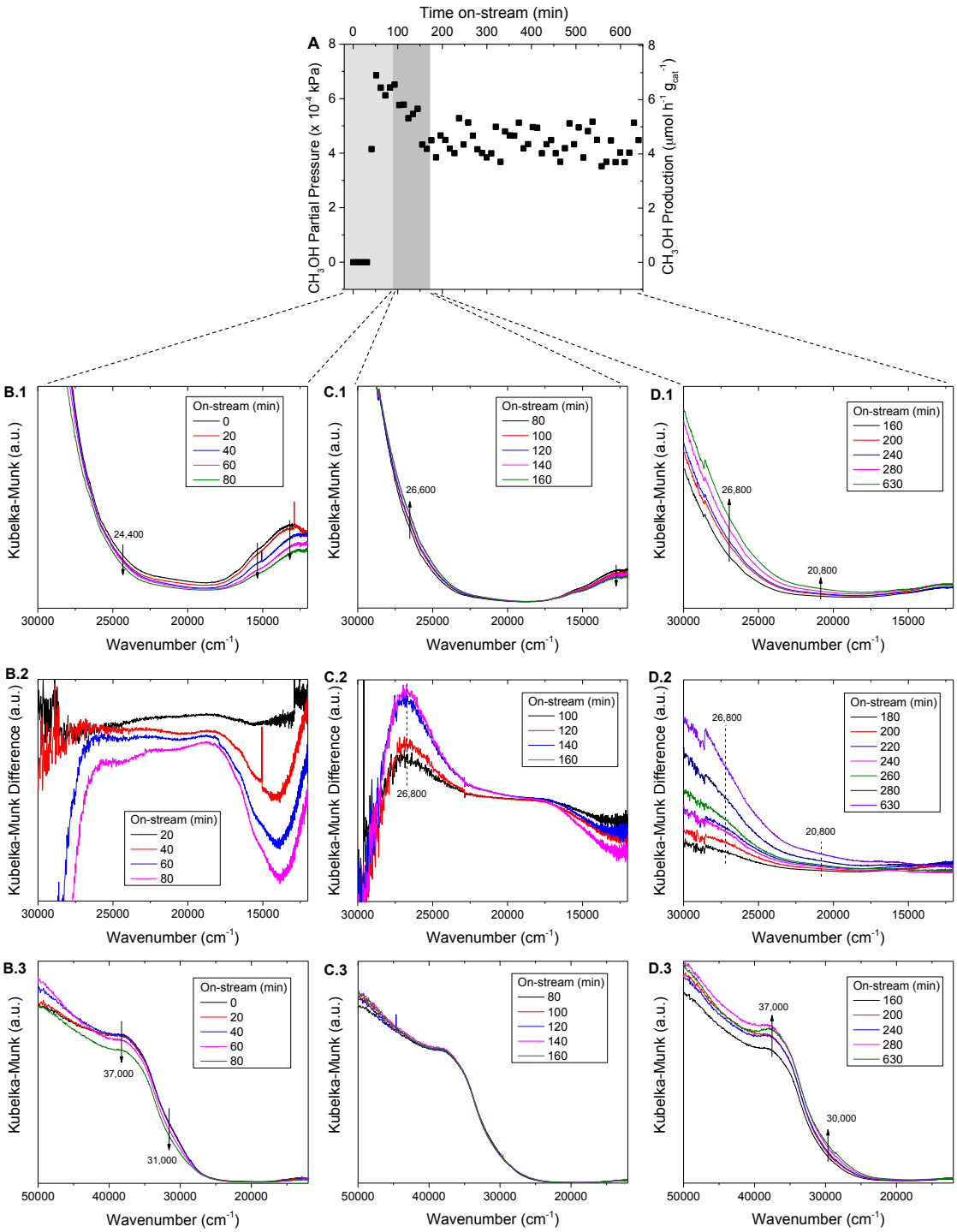

Figure S15. Combined in-situ diffuse reflectance UV-visible spectroscopy and online gas chromatography measurements for catalytic CH_4 oxidation over Cu-Na-ZSM-5 (Cu/Al = 0.37). Catalyst pretreatment: heating to 823 K under flowing O_2, 2 h at 823 K under He, cooled to 483 K under flowing He. Initial CH_4 oxidation: 0.5 h under 25000 mL h^{-1} g_{cat}^{-1} of CH_4 at 483 K. Reaction conditions: T = 483 K, WHSV = 25000 mL h^{-1} g_{cat}^{-1}, P_{CH4} = 93.2 kPa, P_{H2O} = 3.2 kPa, P_{O2} = 0.051 kPa. (A) CH_3OH production from Cu-Na-ZSM-5 measured by gas chromatography. (B.1-B.3) diffuse reflectance UV-vis spectra of the 0-80 min time on-stream interval corresponding to the onset of stoichiometric CH_3OH production. The difference spectra in (B.2) subtracts the spectrum at 0 min from each spectrum in the 20-80 min time on-stream interval. (C.1-C.3) diffuse reflectance UV-vis spectra of the 80-160 min time on-stream interval corresponding to the end of stoichiometric and the onset of

steady-state CH_3OH production. The difference spectra in (C.2) subtracts the spectrum at 80 min from each spectrum in the 100-160 min time on-stream interval. (D.1-D.3) diffuse reflectance UV-vis spectra of the 160-630 min time on-stream interval corresponding to steady-state CH_3OH production. The difference spectra in (D.2) subtracts the spectrum at 160 min from each spectrum in the 180-630 min time on-stream interval.

Section S10: Catalytic CH_4 Oxidation over Cu-ZSM-5 and Cu-MOR Zeolites

Table S1. **CH_4 oxidation over Cu-exchanged ZSM-5 and MOR zeolites**

Material	Framework	Si/Al_{nom} [a]	Co-Cation	Si/Al_{tot} [b]	Cu/Al_{tot} [c]	Specific Activity [d]	STY [e] ($\times 10^{-3}$ h^{-1})	E_a^{app} [f] (kJ/mol)
ZSM-5	MFI	11.5	Na^+	13.1	0.17	0.51	2.7	47 ± 2
				13.6	0.37	0.88	2.2	54 ± 5
			H^+	13.9	0.13	0.84	6.0	88 ± 6
				14.1	0.38	1.51	3.8	80 ± 2
Mordenite	MOR	10	Na^+	11.4	0.14	0.30	1.8	92 ± 3
			H^+	11.1	0.14	0.84	4.6	149 ± 2

Catalyst pretreatment: 5 h at 823 K under flowing $O_{2,}$, cooled to 483 K under O_2 flow and then purged under He for 0.5 h. Initial CH_4 oxidation: 0.5 h under 2400 mL h^{-1} g_{cat}^{-1} CH_4. Reaction conditions: T = 483 K, WHSV = 2400 mL h^{-1} g_{cat}^{-1}, P_{CH4} = 98.1 kPa, P_{H2O} = 3.2 kPa, P_{O2} = 0.0025 kPa (25 ppm). ± denotes 95% confidence intervals

[a] nominal ratio of silicon to aluminum atoms in each zeolite based on commercial figures.
[b] ratio of total silicon to aluminum atoms in each zeolite sample. Determined using inductively coupled plasma mass spectrometry (ICP-MS).
[c] ratio of total copper to aluminum atoms in each zeolite sample. Determined using ICP-MS.
[d] specific activity is defined as μmol_{CH3OH} h^{-1} g_{cat}^{-1}.
[e] Site-time yield (STY) is defined as mol CH_3OH (mol Cu)$^{-1}$ h^{-1}.
[f] E_a^{app} is defined as apparent activation energy (kJ/mol).

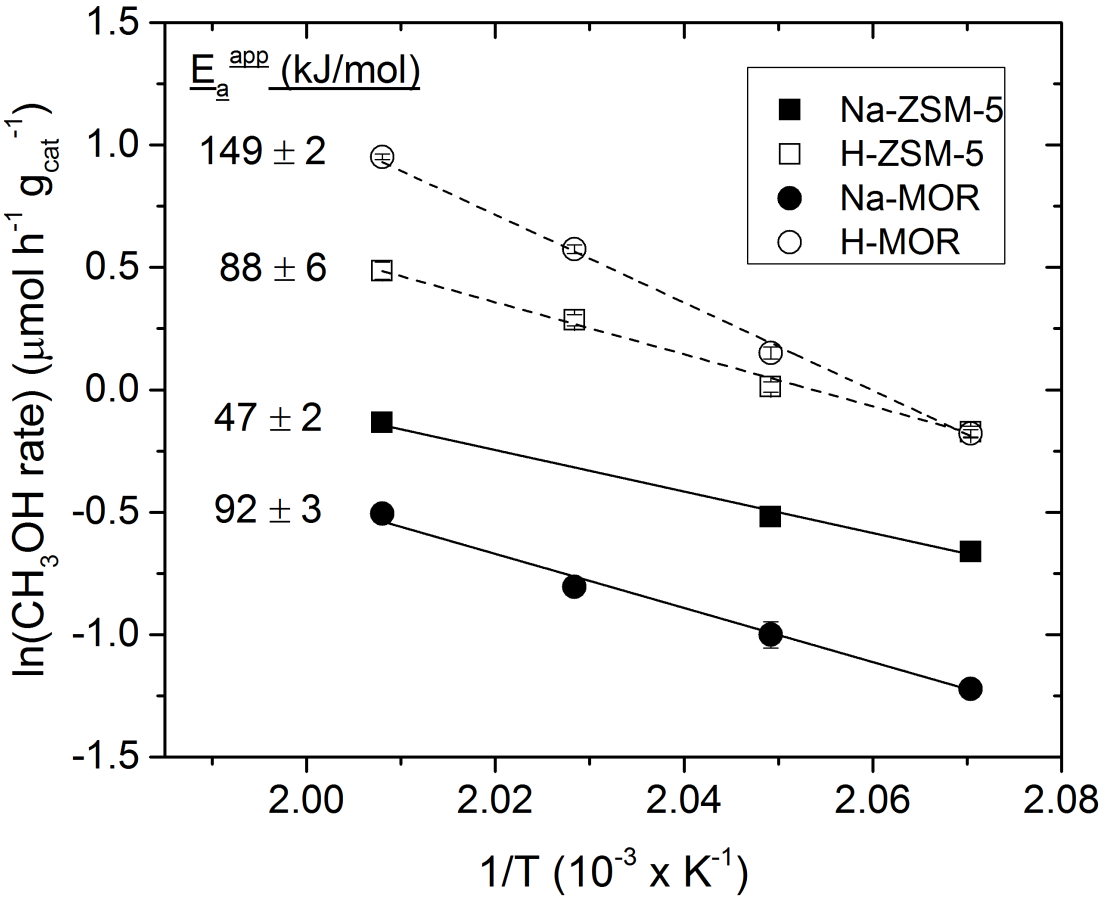

Figure S16. Arrhenius plot of catalytic CH_4 oxidation over Cu-ZSM-5 and Cu-MOR zeolites.

Open symbols: zeolites with Brønsted acid sites (ZSM-5 had Cu/Al = 0.13, MOR had Cu/Al = 0.14). Closed symbols: zeolites with sodium as counter ions (ZSM-5 had Cu/Al = 0.17, MOR had Cu/Al = 0.14). Catalyst pretreatment: 5 h at 823 K under flowing O_2, cooled to 483 K under O_2 flow and then purged under He for 0.5 h. Initial CH_4 oxidation: 0.5 h under 2400 mL h^{-1} g_{cat}^{-1} CH_4. Reaction conditions: T = 483 K, WHSV = 2400 mL h^{-1} g_{cat}^{-1}, P_{CH4} = 98.1 kPa, P_{H2O} = 3.2 kPa, P_{O2} = 0.0025 kPa (25 ppm). E_a^{app} = apparent activation energy in kJ/mol for each zeolite. ± denotes 95% confidence intervals

Section S11: CH_4 Oxidation vs. Temperature over Cu-Na-SSZ-13 (Cu/Al = 0.50)

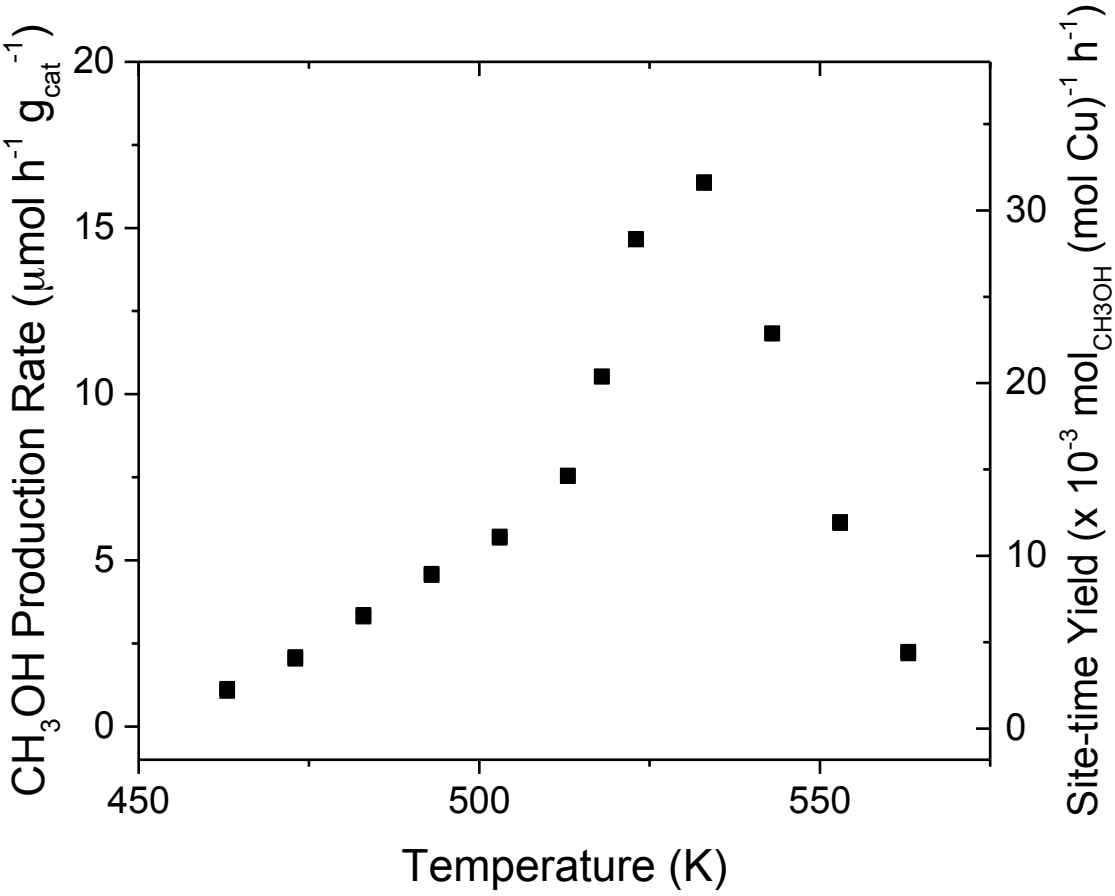

Figure S17. Catalytic CH_4 oxidation over Cu-Na-SSZ-13 (Cu/Al = 0.50) as a function of reaction temperature.
Catalyst pretreatment: 5 h at 823 K under flowing O_2, cooled to 483 K under O_2 flow and then purged under He for 0.5 h. Initial CH_4 oxidation: 0.5 h under 2400 mL h^{-1} g_{cat}^{-1} CH_4. Reaction conditions: WHSV = 3600 mL h^{-1} g_{cat}^{-1}, P_{CH4} = 88.9 kPa, P_{H2O} = 3.2 kPa, P_{O2} = 0.088 kPa, He balance. Error bars denote 95% confidence intervals.

Section S12: CH_4 Oxidation over CuO_x-Zeolites Prepared by Incipient Wetness Impregnation

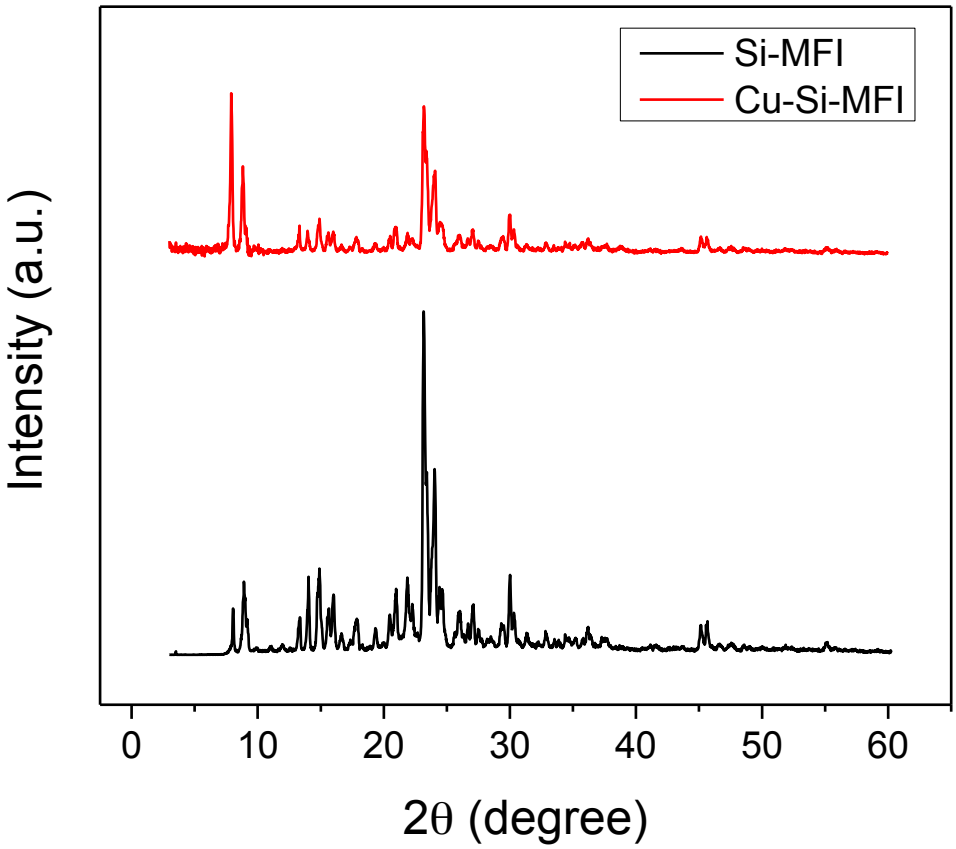

Figure S18. Powder x-ray diffraction pattern of CuO_x-Si-MFI (1.1 wt% Cu). No reflections for CuO nor Cu_2O could be detected in the diffraction pattern.

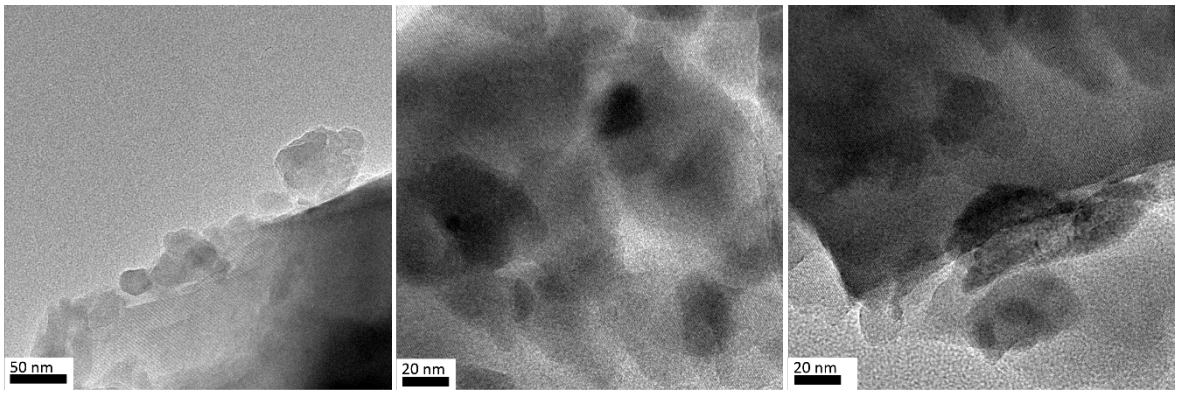

Figure S19. TEM Images of CuO_x-Si-MFI (1.1 wt% Cu). Large CuO_x particles are observed with average size 30 ± 20 nm.

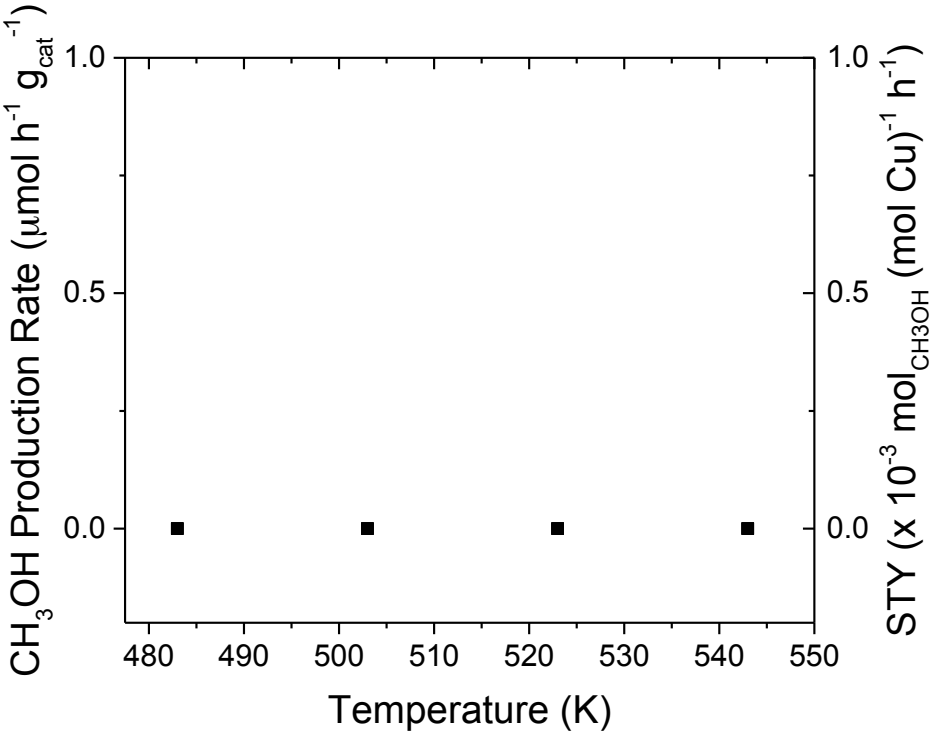

Figure S20. Catalytic CH_4 oxidation over CuO_x-MFI (1.1 wt% Cu) as a function of reaction temperature.

Catalyst pretreatment: 5 h at 823 K under flowing O_2,, cooled to 483 K under O_2 flow and then purged under He for 0.5 h. Initial CH_4 oxidation: 0.5 h under 2400 mL h^{-1} g_{cat}^{-1} CH_4. Reaction conditions: WHSV = 2400 mL h^{-1} g_{cat}^{-1}, P_{CH4} = 93.1 kPa, P_{H2O} = 3.2 kPa, P_{O2} = 0.051 kPa, He balance.

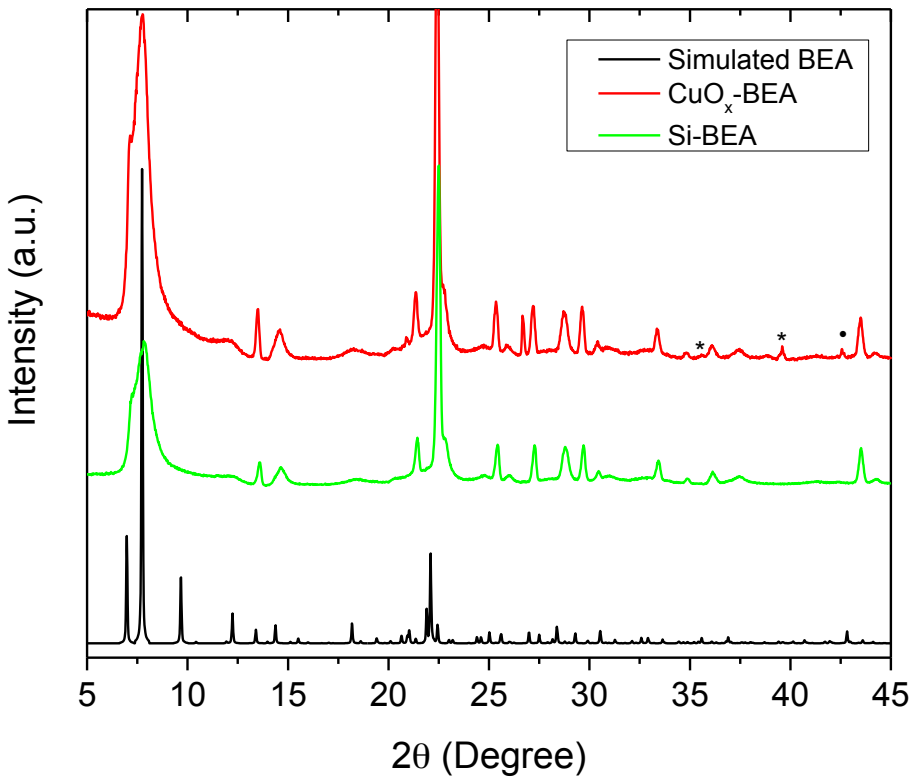

Figure S21. Powder x-ray diffraction patterns of CuO_x-BEA (1.1 wt% Cu).
* denotes reflections of CuO and • denotes reflections of Cu_2O.[9] The average CuO particle size was estimated to be 41 nm for CuO ($2\theta = 39.6^{\circ}$) and 60 nm for Cu_2O ($2\theta = 42.6^{\circ}$) using the Sherrer equation.

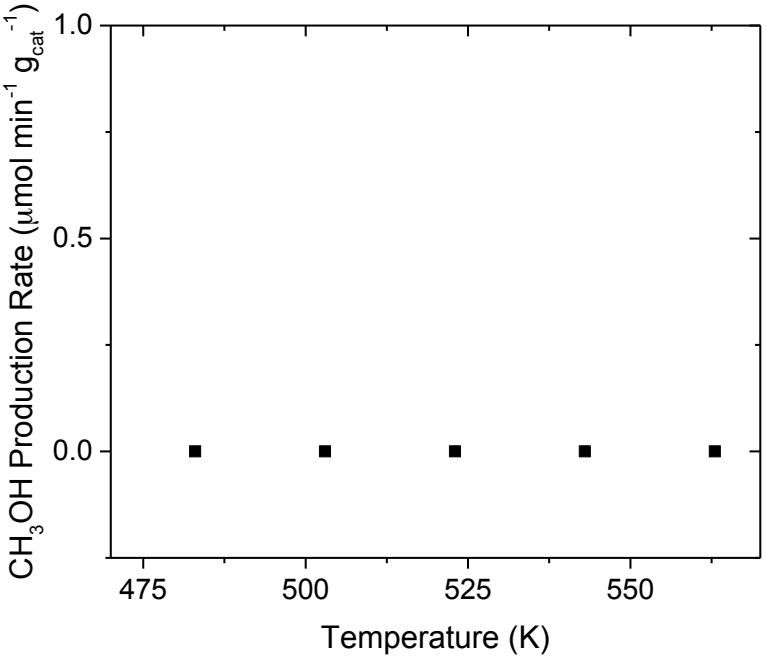

Figure S22. Catalytic CH_4 oxidation over CuO_x-BEA (1.1 wt% Cu) as a function of reaction temperature.
Catalyst pretreatment: 5 h at 823 K under flowing O_2,, cooled to 483 K under O_2 flow and then purged under He for 0.5 h. Initial CH_4 oxidation: 0.5 h under 2400 mL h^{-1} g_{cat}^{-1} CH_4. Reaction conditions: WHSV = 2420 mL h^{-1} g_{cat}^{-1}, P_{CH4} = 93.1 kPa, P_{H2O} = 3.2 kPa, P_{O2} = 0.051 kPa, He balance.

Section S13: Materials Characterization

Table S2. Elemental composition, pore volume and surface area analysis (BET) of Cu-exchanged zeolites

Material[a]	Framework	Si/Al[b]	Si/Al_{tot}[c]	Cu/Al[d]	Cu wt%[e]	Fe/Al[f]	V_{micro} (cm^3 g_{cat}^{-1})[g]
Na-ZSM-5	MFI	11.5	13.6	0.37	2.5	0.01	0.14
Na-ZSM-5	MFI	11.5	13.1	0.17	1.2	0.01	0.14
H-ZSM-5	MFI	11.5	13.2	0.31	2.2	0.01	0.14
H-ZSM-5	MFI	11.5	13.9	0.13	0.9	0.01	0.15
H-ZSM-5	MFI	11.5	12.9	0	0	0.00	0.16
Na-MOR	MOR	10	11.4	0.14	1.1	0.01	0.17
H-MOR	MOR	10	11.1	0.14	1.1	0.01	0.19
H-MOR	MOR	10	10.4	0	0	0.00	0.20
Na-SSZ-13	CHA	15	13.8	0.50	3.3	0.00	0.24

[a] zeolite material with parent counter cation form before copper-exchange. Na denotes sodium form, H denotes proton form.
[b] nominal ratio of total silicon to aluminum atoms in the zeolite based on commercial figures or ratios of SiO_2 to Al_2O_3 in synthesis procedures.
[c] calculated ratio of total silicon to aluminum atoms in the zeolite. Quantified using inductively coupled plasma mass spectrometry (ICP-MS).
[d] calculated ratio of total copper to aluminum atoms in copper-exchanged zeolite. Quantified using ICP-MS.
[e] weight percent of copper in copper-exchanged zeolite.
[f] calculated ratio of total iron to aluminum atoms in copper-exchanged zeolite. Quantified using ICP-MS. Fe/Al was quantified to provide an estimate of iron impurities in copper-exchanged zeolites.
[g] micropore volume of copper-exchanged zeolites determined by BET analysis.

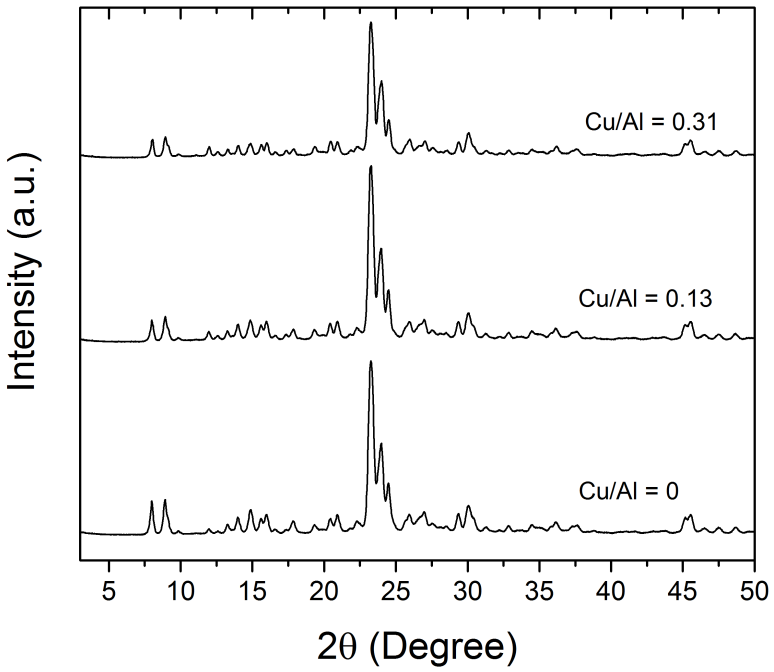

Figure S23. Powder x-ray diffraction patterns of Cu-exchanged H-ZSM-5 (Si/Al = 12.9 – 13.9) catalysts.
After ion exchange, drying, and calcination, no reflections were observed corresponding to copper or copper oxide particles (< 3 nm)

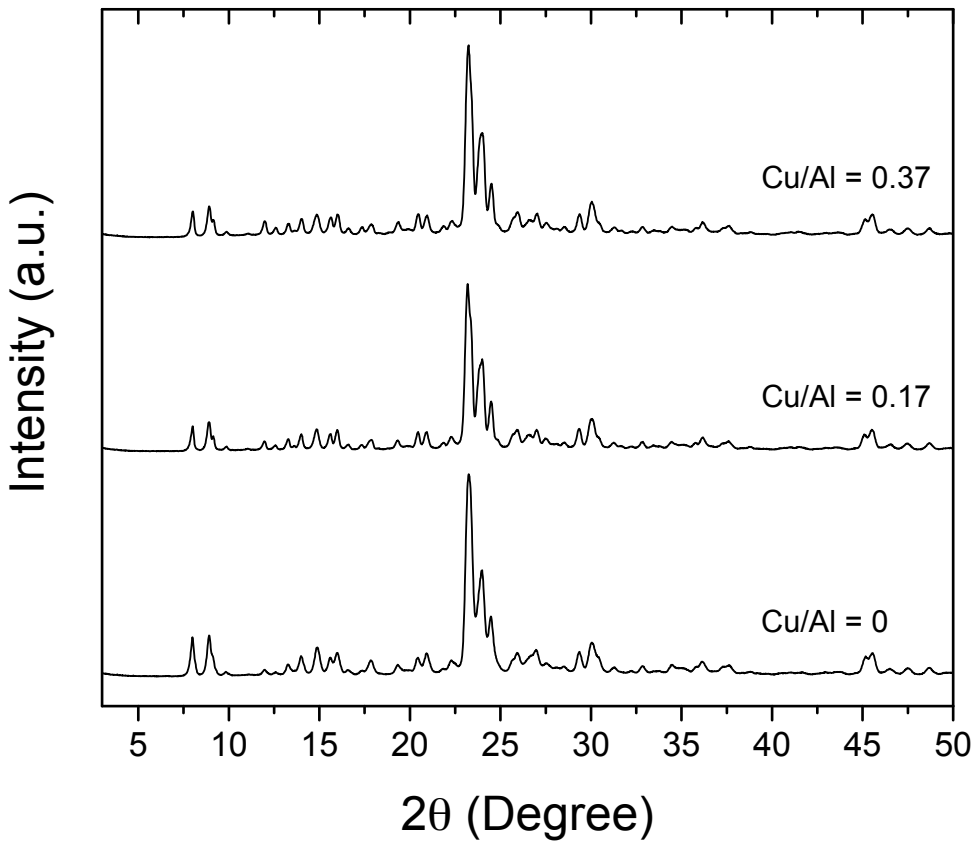

Figure S24. Powder x-ray diffraction patterns of Cu-exchanged Na-ZSM-5 (Si/Al = 12.9 – 13.6) catalysts.
After ion exchange, drying, and calcination, no reflections were observed corresponding to copper or copper oxide particles (< 3 nm)

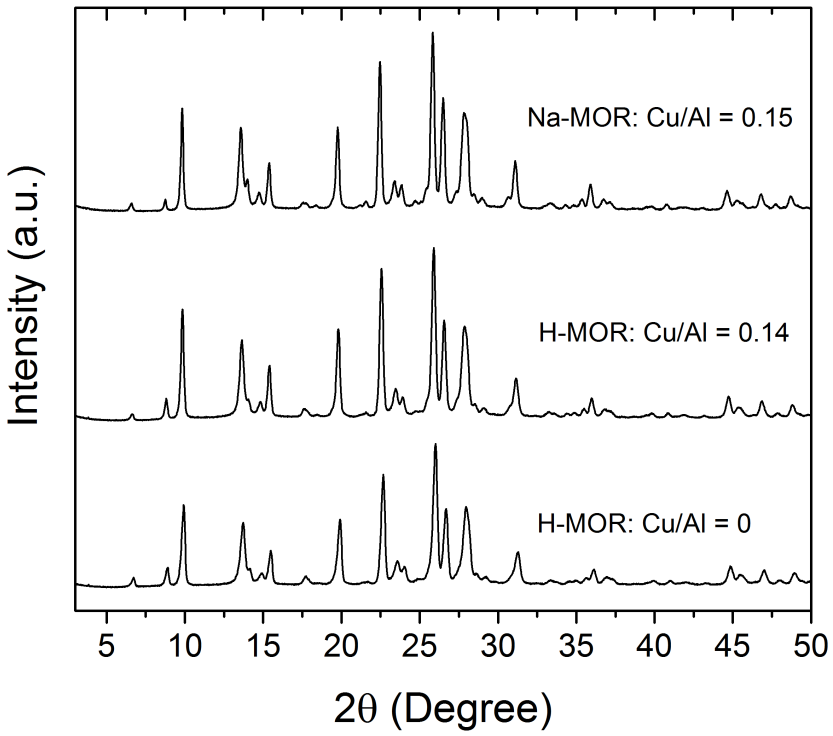

Figure S25. Powder x-ray diffraction patterns of Cu-exchanged MOR (Si/Al = 10.4 – 11.4) catalysts.

After ion exchange, drying, and calcination, no reflections were observed corresponding to copper or copper oxide particles (< 3 nm)

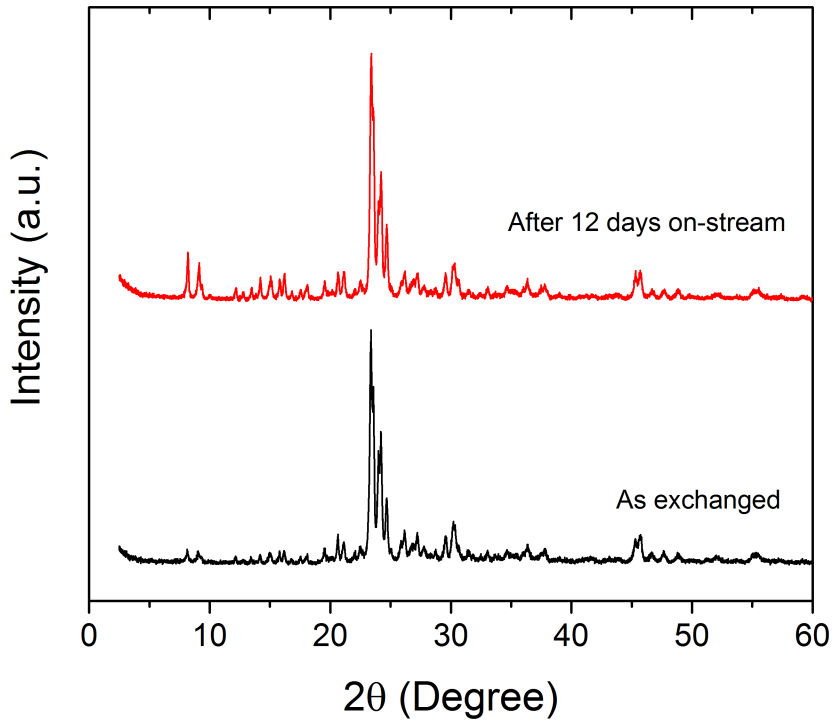

Figure S26. Powder x-ray diffraction of Cu-H-ZSM-5 (Cu/Al = 0.31) after exchange and after CH_4 oxidation for 12 days-on-stream.

References

(1) Camblor, M. A.; Corma, A.; Valencia, S. Spontaneous nucleation and growth of pure silica zeolite-β free of connectivity defects. *Chem. Commun.* **1996**, 2365-2366.
(2) Persson, A.; Schoeman, B.; Sterte, J.; Otterstedt, J.-E. The synthesis of discrete colloidal particles of TPA-silicalite-1. *Zeolites* **1994**, *14*, 557-567.
(3) Baerlocher, C.; McCusker, L. B. Database of Zeolite Structures. http://www.iza-structure.org/databases/
(4) Yaripour, F.; Baghaei, F.; Schmidt, I.; Perregaard, J. Catalytic dehydration of methanol to dimethyl ether (DME) over solid-acid catalysts. *Catal. Commun.* **2005**, *6*, 147-152.
(5) Blaszkowski, S. R.; van Santen, R. A. The mechanism of dimethyl ether formation from methanol catalyzed by zeolitic protons. *J. Am. Chem. Soc.* **1996**, *118*, 5152-5153.
(6) Wang, W.; Seiler, M.; Hunger, M. Role of surface methoxy species in the conversion of methanol to dimethyl ether on acidic zeolites investigated by in situ stopped-flow MAS NMR spectroscopy. *J. Phys. Chem. B* **2001**, *105*, 12553-12558.
(7) Hassanpour, S.; Yaripour, F.; Taghizadeh, M. Performance of modified H-ZSM-5 zeolite for dehydration of methanol to dimethyl ether. *Fuel Process. Technol.* **2010**, *91*, 1212-1221.
(8) Vishwanathan, V.; Jun, K.-W.; Kim, J.-W.; Roh, H.-S. Vapour phase dehydration of crude methanol to dimethyl ether over Na-modified H-ZSM-5 catalysts. *Appl. Catal., A* **2004**, *276*, 251-255.
(9) Song, Q.; Liu, W.; Bohn, C. D.; Harper, R. N.; Sivaniah, E.; Scott, S. A.; Dennis, J. S. A high performance oxygen storage material for chemical looping processes with CO2 capture. *Energy Environ. Sci.* **2013**, *6*, 288-298.